Cell cycle distribution and CKS2 protein content in cervical carcinoma cell lines after exposure to ionizing radiation

A dissertation in cell biology for the cand.pharm degree

by Eli Faksvåg Caspersen

Rikshospitalet-Radiumhospitalet Medical Centre
School of Pharmacy
Faculty of Mathematics and Natural Sciences
University of Oslo
Autumn 2006

TABLE OF CONTENTS

ACKNOWLEDGEMENTS

The present work was carried out at the Department of Radiation Biology, Institute for Cancer Research at Rikshospitalet-Radiumhospitalet Medical Centre from November 2005 to November 2006.

I would like to thank my supervisor, Heidi Lyng, for her advice and patience. I am grateful for the way you have shared your knowledge. I would also like to thank Trond Stokke for many interesting discussions, and the whole research group for making me feel as part of them.

Kirsten Skarstad commented my work in the final stages of the writing process, for which I am grateful.

Anne Katrine Hindhammer and Håvard Kirkevold have been invaluable this past year. Thank you, Anne, for the work we did together, and thank you both for the laughs and drinks we have had so far.

All the kindness and encouragements from other friends and family has also been highly appreciated. It is strange how you never seem to lose your faith in me.

Last, I would like to thank Trond Méthi. You make my days brighter.

Oslo 12.11.2006 Eli Faksvåg Caspersen

ABSTRACT

Cervical cancer is one of the major causes of gynecological death worldwide. The degree of cancer progression of is categorized into different stages. Therapy is given depending on the stage of the cancer. Radiation is the main therapy in the advanced stages. Unfortunately, radiation therapy also causes severe damage to normal tissue. A better understanding of the cellular responses to radiation is needed to improve therapy.

Analysis of cell material from patients with cervical cancer can show differences in gene expression. Upregulated expression of the CKS2 gene is associated with high malignancy and poor patient survival. CKS2 could serve as a therapeutic marker and a possible new target for chemotherapeutic drugs. Determining the role of the CKS2 protein in radiation response may therefore contribute to improve therapy.

Two immortalized cervical carcinoma cell lines, Hela and Siha, were used in the experiments in this thesis. Preliminary work included establishing cell line characteristics with respect to growth, plating efficiency and radiosensitivity. Effect of radiation on cell cycle distribution was determined 24 hours after various doses and at different times after irradiation with 8Gy. A method for detecting CKS2 protein content in the cell was developed. The analyses were performed with flow cytometry. A developed staining procedure allowed us to observe the CKS2 protein content in the different phases of the cell cycle individually. Attempts were made to localize the CKS2 protein in the cells. Potential changes in CKS2 protein conformation in the cell cycle were also investigated.

The doubling time was 22 hours for Hela cells and 34 hours for Siha cells. The plating efficiency found for Hela was 49 % and for Siha 45 %. Hela cells were found to be more radiosensitive than the Siha cells, and the difference was significant even at low radiation doses. Further results show that the cervical carcinoma cells from both cell lines were arrested in G2 phase 4 hours after irradiation. The fraction of cell arresting in G2 was increasing with increasing radiation doses. The lowest radiation dose that caused a significant increase in cell fraction in G2-M in both cell lines was 4 Gy. The G2 arrest

was abolished 30 and 48 hours after irradiation for Hela and Siha cells, respectively, and the cells reentered the cell cycle.

The CKS2 protein content increased in all phases for both cell lines 6-24 hours after irradiation, but the increase was only significant in M phase. In Siha cells, there was no change in CKS2 protein content at times after 24 hours. For Hela cells there was a decrease followed by a second significant increase after 48 hours. In Siha cells, a significant increase in CKS2 protein content was also detected in G2 phase after 30-48 hours. An increase in CKS2 protein content in M phase was seen in Hela cells with increasing radiation doses. The first significant increase was detected after 4 Gy, and a further increase was detected after 10 Gy. There was also an increase in G2 phase after 4 Gy, from which there was no further change. In Siha cells, a significant increase in CKS2 protein content is only detected in M phase after 8 Gy.

Linking CKS2 protein content to cell cycle distribution was attempted, but further research must be done to clarify the role of CKS2 in radiation response. The localization of the CKS2 protein in the cell was illustrated. Findings that indicated conformational changes between interphase and M phase were also presented. The results can provide useful information for further work with the cervical carcinoma cell lines and their responses to radiation. The CKS2 findings may contribute to a better understanding of the functions of this protein in the cell. As a small part of a larger picture, this work could have an impact on improving therapy for cervical cancer patients.

ABBREVIATIONS

BP – Band Pass

Cdk – Cyclin Dependent Kinases

CDKI – Cyclin Dependent Kinase Inhibitors

CIN – Cervical Intraepithelial Neoplasia

CKS2 – CDC28 Protein Kinase Regulatory Subunit 2

DMSO - Dimethyl Sulfoxide

DSB – Double Strand Breaks

EDTA – Ethylenediaminetetraacetic acid

FIGO – International Federation of Gynaecology and Obstetrics

FITC – Fluorescein Isothiocyanate

FSC – Forward Scatter

Gy – Gray

HPV – Human Papilloma Virus

LFM – “Larsen”-Formaldehyde-Methanol

LP – Long Pass

PBS – Phosphate Buffer Saline

PE – Phycoerythrin

PE – plating efficiency

PH3 – Phosphorylated Histone H3

PI – Propidium Iodide

PMT – Photo Multiplier Tube

RB1 – Retinoblastoma

SF – Survival Fraction

SP – Short Pass

SSC – Side Scatter

INTRODUCTION

Cancer is recognized by abnormal cell proliferation [1]. The cells that are dividing at an increased rate have lost parts of their control system regulating growth and cell division. Viral infections can in part contribute to the loss of function of crucial cell cycle regulators. Cervical cancer is one of the most common cancers affecting women worldwide and the mortality rates are high [2-4]. DNA from high-risk types of HPV is detected in over 90 % of all cervical cancers [5-7]. These HPV types are known to code for proteins capable of disrupting important regulators of the cell cycle, such as TP53 and RB1.

Offered therapy after diagnosis of cervical cancer depends on the stage, but radiation is the most widely used treatment to the advanced stages [2;8]. Unfortunately, the radiation therapy also causes significant damage to normal tissue. To improve therapy, a better understanding of cellular responses to radiation is needed. This could lead to the discovery of new targets for chemotherapeutics. It can also lead to detection of therapeutic markers that potentially can be used to sort out patients with need of a more aggressive therapy.

Cell material from patients with cervical cancer is analyzed as a part of a larger project. These samples are screened for differences in expression of many genes, and these differences are seen in relation to the malignancy of the tumor and patient survival [9]. Genes that are upregulated and associated with malignancy and poor patient survival may code for proteins that potentially could be new therapeutic targets or –markers. One protein showing promising results is the CKS2 protein.

Little is known about the functions the CKS2 protein has in the cell. A greater understanding of the CKS2 proteins role in the cell cycle is needed. The potential role for the CKS2 protein in radiation response also needs further examining to determine this proteins potential for improving therapy.

The initial purpose for the experiments in this thesis was to establish two immortal cervical carcinoma cell lines, Hela and Siha, in the department laboratory. The cell lines were infected with two different types of high-risk HPV and originated from the two most common cervical cancer types. Their growth rate, plating efficiency and radiosensitivity had to be determined before they could be used in radiobiological studies. This work was done in collaboration with another student.

Further experiments would search for potential changes in cell cycle distribution in response to radiation in the two established cell lines. The fractions of cells in the different parts of the cycle would be determined after different radiation doses and different times after radiation.

After phenotypic response to radiation in the two cell lines had been determined, the CKS2 protein content in the carcinoma cell lines could be observed. A method for detecting the CKS2 protein had to be developed. The potential changes in cellular CKS2 protein content would then be measured for each phase of the cycle separately after different radiation doses and after different times. Using different methods for fixating cells, it could also be possible to comment on changes in conformation of the CKS2 protein in the cell in the different parts of the cell cycle.

The main analysis method used for determining changes in cell cycle distribution, CKS2 protein content and conformational changes of the protein during cycle, was flow cytometry.

BACKGROUND

1.1 Cell cycle and regulation in mammalian cells

1.1.1 The cell cycle

The cell cycle is traditionally divided into four sequential phases: the G1, S, G2 and M phase (figure 1) [10]. The three first are collectively known as the interphase. M phase can be further divided into mitosis and cytokinesis. There are also further subdivisions of phases in the mitosis.

In the S phase the entire DNA in the cell is duplicated. This normally requires 10-12 hours and occupies approximately half the time spent in the cell cycle in a typical mammalian cell. In the M phase the two sister chromatides are pulled apart in the mitosis, whereas the actual cell division takes place in the cytokinesis. The M phase takes much less time than S phase; less than an hour in a normal mammalian cell. The cell enters G1 and arrest if it does not receive the appropriate signals from its environment. From G1, the cell can even enter a specialized resting state called G0 in which it can stay for days, months or even years. If a cell in G0 receives appropriate signals, it can reenter the cycle. In G2, the cells major concern is to enlarge its mass for the following cell division.

These sequential phases are the basis for creating two identical daughter cells, which are also identical to their progenitor, with respects to size and content. There are regulatory control mechanisms that make sure that cells are only proliferating when it is beneficial.

1.1.2 Regulation of the cell cycle

There are many control mechanisms that closely monitor and regulate all processes in the cell cycle. These mechanisms are represented by three distinct checkpoints in each cell cycle (figure 1).

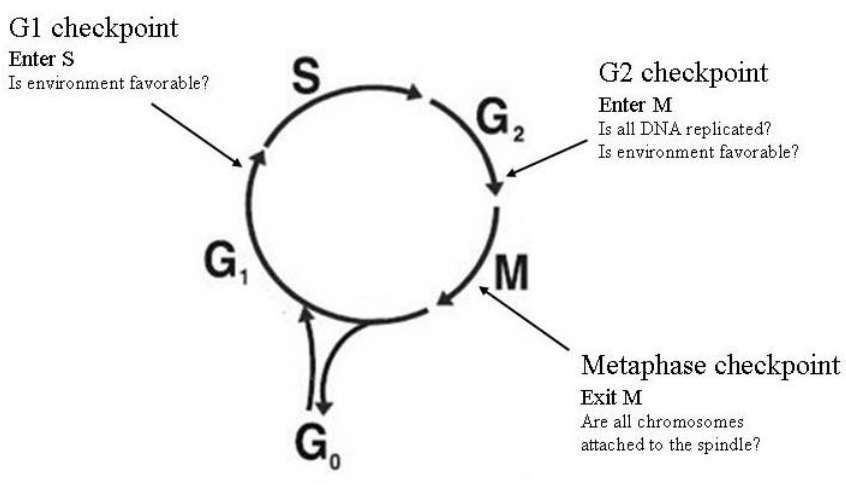

Figure1. *G1 and G2 are gap phases. S phase stands for synthesis, indicating the full replication of the DNA in this phase. M phase stands for mitosis, the part of the phase when the chromosomes are propelled apart after attachment to the two spindles localized in each pole of the cell, and separated into two daughter cells. Even though M phase has its name from mitosis, cytokinesis is also a part of it. The checkpoints in G1, S and G2 phase are indicated.*

The G1 checkpoint is also called the restriction point or the point of no return since if the cell passes this point it commits to one full cycle. The checkpoints can be activated by several pathways depending on the stress that the cell is exposed to [11]. The upstream regulators of the checkpoints will vary depending on the stress, whether the cause is DNA damage, hypoxia or other factors. However, the end result will always be the same; a delay or arrest of the cell cycle while mechanisms attempting to repair the damage are mobilized. A complete arrest of the cell cycle only happens in the checkpoints, while retardation can occur in all phases. If the damage is too severe and repair is not possible, other cellular processes will start up making sure that abnormal cells will not divide and/or survive.

The cell cycle is driven by the cyclin dependent kinases (Cdks) and their activating coenzymes; the cyclins (figure 2) [10;12]. The kinase activities of the Cdks are affected by the accessibility to their respective cyclin(s) and their interaction with CDKIs, phosphatases and activating/inhibitory kinases.

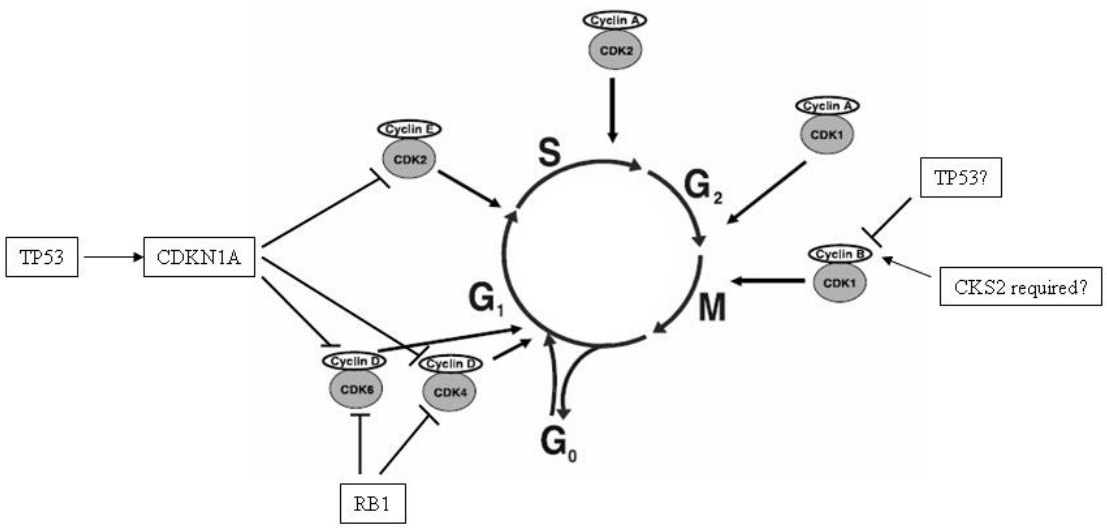

Figure 2. *An illustration of some of the most important regulators in the different parts of the cell cycle in addition to the Cdks with their corresponding cyclins and their sites of action.(modified from [13])*

Mitogens will signal to the cell in G0 or G1 phase if cell proliferation is needed for tissue homeostasis. The mitogens interact with the cell, causing intracellular signaling molecules to drive the cell cycle forward and beyond the restriction point.

Active RB1 (pRb) protein will repress transcription of genes for many proteins necessary for passage through the restriction point [10;12]. Inactivating RB1 is therefore crucial for cell cycle progression.

Low concentrations of TP53 (p53) are normally detected in non cycling cells. The low levels are due to TP53s interaction with another protein which targets TP53 molecules for degradation. In response to stress, TP53's binding to this protein is reduced. The levels increase and TP53 is activated. In its activated form, TP53 acts as a transcription regulator. It is responsible for the transcription of several genes coding for proteins such as CDKN1A (p21) and CCNB (cyclin B). Increased CDKN1A and CCNB transcription leads to potential G1- or G2 delay/arrest. TP53 is also a major mediator for programmed cell death, apoptosis [10]. Cells with mutated or otherwise unfunctional TP53 and/or RB1 loose their fidelity to the checkpoints. Additionally, apoptosis will not be mediated in an

appropriate manner with a loss of TP53 function. Many cancerous cells have found to have unfunctional TP53 and/or RB1 [1;13].

It has been suggested that an association of the CKS2 protein to the CDC2/CCNB complex is somehow involved in the activating dephosphorylation needed for passage through the G2-M phase transition [14;15]. The role of CKS2 is, however, unclear. CKS2 (analogues) is/are observed to be bound to mitotic cyclin-dependent kinase in yeast, human cells and frog eggs [15]. In frog eggs, the human CKS2 protein binds with high preference to the activated CDC2/CCNB [14]. A CKS2 homologue is also found in plant cells, localized in the nucleus as long as the nuclear envelope is intact. At the onset of M-phase, the protein diffuses to all the parts of the cells uniformly [16]. CKS2 gene expression is found to have a positive significant correlation with cell proliferation in patients with lymphoid malignancies [17]. Mice lacking CKS2 protein are found to be sterile. The suggested reason for this is a necessity of CKS2 for progression through the first metaphase in meiosis [18]. This may be of relevance since the first cell division in meiosis is similar to that of mitosis.

Due to the protective qualities of TP53 and RB1 against cancer, the genes coding for them are categorized as two of many tumor suppressor genes. In contrast, genes that code for proteins that promote cancer are called oncogenes and oncoproteins, respectively [1].

1.2 Cancer

When the cell cycle regulation mechanisms for some reason are disrupted, cell proliferation can occur when it is not favorable [1]. Abnormal cells will divide too frequently and create a relentlessly growing mass, a tumor, where each cell passes this abnormality to their progeny. If the cells in a tumor hold together in a single mass, it is said to be benign. The cancerous cells can start invading the tissue surrounding the initial tumor. If the cells in a tumor develop the ability of invading the surrounding tissue, the tumor is malignant. Cancerous cells can dislodge from the tumor, enter the bloodstream or lymphatic vessels and form secondary tumors called metastases. Invasiveness usually

implies the ability of metastasis formation. Malignant tumors are also referred to as cancers.

Much is unclear concerning causes for failure of the regulatory mechanisms, however some have been identified. Genetic defects causing errors in transcriptional activity is the major potential hazard for tumor development. These defects can be caused by gene mutations, -amplifications or –deletions in addition to viral infections. Viral infections contribute to genomic instability by introducing viral DNA or RNA to the cell. The viral DNA or RNA can, by incorporating itself into the host cell DNA, disrupt crucial parts for transcription. It can also serve as template for production of proteins that may have the ability of eliminating parts of the cell cycle regulating system.

Cancers are classified according to the type of tissue in which they first originated. Carcinomas are cancers arising from epithelial cells.

Immortalized cell lines derived from cancers are used as parts of model systems in scientific research. They make it possible to observe the cellular responses after exposure to various stresses. Results found in these model systems can be indicative of the effects of treatment in patients. This gives useful information for better understanding the nature of cancerous cells and can be used to improve existing cancer therapy.

1.2.1 Cervical cancer

Cervical carcinoma is a collective term for various histological cancer types where squamous cell carcinoma, originating from the squamous epithelium (figure 3b), is the most common representing approximately 90 % of the cases [2]. Adenocarcinoma, originating from the columnar epithelium (figure 3b), is the second largest class with close to 10 % of the cases.

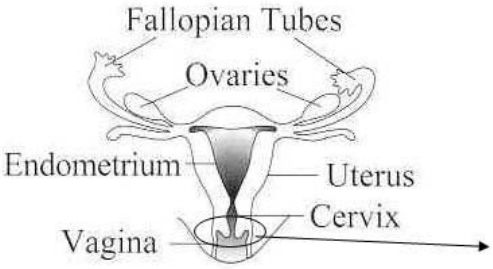

Figure 3a. *Overview of the female reproductive system [19]*

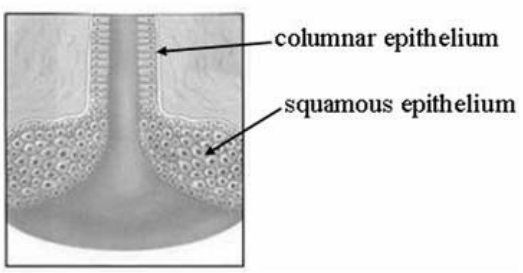

Figure 3b. *Normal cells [20]*

1.2.2 HPV and its influence on cell cycle

HPV is a small nonenveloped double stranded DNA virus [21] from which over 70 individual types has been recognized. HPV is a commonly sexually transmitted virus; approximately 80 % of all women are infected in their lifetime [22]. High-risk HPV types have DNA coding for oncoproteins with greater ability of interacting with tumor suppressor genes and regulatory proteins in the cell compared to the low-risk kinds, and are therefore associated with a higher cancer risk [6]. Two of the high-risk types are HPV 16 and HPV 18; DNA from these is found in over 90 % of all cases of cervical cancer and precursor lesions [5-7].

The two main oncoproteins produced from the HPV DNA are E6 and E7 [23;24]. Their expression is highly increased after integration of the viral DNA into the host cell genome [6].

In cervical carcinomas, TP53 is almost invariably wild type. Even so, its function seem to be missing as a regulator of cell cycle, despite that large quantities of TP53 mRNA can be detected in HPV transformed cell lines [21]. The cause for this is the oncoprotein encoded for in the viral DNA, E6, which inactivates and degrades TP53 [6;7;23;24].

Cells expressing HPV 16 or -18 lose their G1 checkpoint quite early [23]. E6 mediated TP53 degradation is the main cause for this; the G1 restriction point is overcome without receiving mitogenic signals and after DNA damage. It is also proposed that the TP53 degradation mediated by E6 is one way of promoting reduced fidelity to control mechanisms associated with entrance to M phase through the G2 checkpoint [24].

E7 has the ability of inactivating RB1 and target it for degradation [6;24]. It can also interact with CDKN1A and prevent its inhibitory functions on CCNE (cyclin E) and CCND (cyclin D) and their associated kinases activity, thereby promoting G1/S transition and DNA replication [25]. E7's interaction with RB1 and CDKN1A contributes to the cell overcoming its G1 restriction point.

Another feature of E7 is the ability of binding to CCNA (cyclin A), resulting in a prolonged S phase [6]. Both E6 and E7 have shown to have impact on the mitotic assembly checkpoint, but with different kinetics [24].

1.2.3 Cervical tumorigenesis and treatment

Cervical tumorigenesis is a multistage process that occurs over time, and cellular abnormalities can be detected at a very early stage. Detected precursor lesions are described as cervical intraepithelial lesions (CIN) [2]. Mild dysplastic changes in the cervical epithelium are described as CIN I, while moderate and severe dysplasia or carcinoma in situ are II and III respectively. In cells from CIN I, low-risk HPV infections are often detected, while in CIN II and III high-risk HPV are often observed. No treatment is required for CIN I, since these lesions often are spontaneously resolved by the immune system. CIN II and III however, require treatment for the prevention of invasive disease. The viral DNA is usually not integrated into its host DNA in CIN, while it is a common feature in invasive cervical cancer.

Microinvasive- or invasive lesions are diagnosed as cervical cancer. The degree of progression of the cervical cancers is described through the clinical staging used

according to the system provided by the International Federation of Gynaecology and Obstetrics (FIGO) [2;4;8]. This staging is shown in table 1.

Table 1. *The staging of cervical cancers provided by FIGO with corresponding treatment and five year survival rates.*

			Therapy *	Five year survival rates
Stage I		The tumor is confined to the uterus		
	IA	Microinvasive disease with the lesion not grossly visible	Surgery	> 95 %
	IB	Larger tumor than in stage IA of grossly visible tumor confined to the cervix	Surgery	80-90 %
Stage II		The tumor extends beyond the uterus, but does not involve the pelvic side wall or lowest third of the vagina		
	IIA	Involvement of the upper two thirds of the vagina, without lateral extension into the parametrium	Surgery Radiation Chemotherapy	80-90 %
	IIB	Lateral extension into parametrial tissue.	Radiation Chemotherapy	65 %
Stage III		The tumor involves the lowest third of the vagina or the pelvic side wall or causes hydronephrosis		
	IIIA	Involvement of the lowest third of the vagina	Radiation Chemotherapy	40 %
	IIIB	Involvement of the pelvic side wall of hydronephrosis	Radiation Chemotherapy	40 %
Stage IV		The tumor demonstrates extensive local infiltration or has spread to a distant site.		
	IVA	Involvement of bladder or rectal mucosa	Radiation Chemotherapy	< 20 %
	IVB	Distant metastasis	Radiation ** Chemotherapy	Incurable

*Therapy refers to the standard protocols at Rikshospitalet-Radiumhospitalet Medical Centre

**Palliative treatment

Different treatments are given for the various stages. Surgery is usually the treatment for stage I cervical cancers. Radiation therapy is the standard treatment if the tumor has reached stages IIB-IV. Additional chemotherapy is offered [8], but since they cause toxicity with side-effects strongly affecting quality of life in addition to lacking documentation of increased survival benefit [2], many patients choose only radiotherapy.

In Norway, 350 women are diagnosed with cervical cancer every year [8;22]. The frequency of cervical cancer diagnoses have been greatly reduced due to screening programs introduced in most countries in the developed world. No equivalent enterprise is performed in most third world countries, and cervical cancer remains one of the most common tumors affecting women and a leading cause of gynecological cancer death worldwide [2-4].

The survival rates are relatively high after receiving treatment for cervical cancer, especially for the early stages where the majority of patients are cured after surgery. Still, improvement of therapy is needed, especially for the higher stages where radiation is the main therapy, since the radiation doses required for controlling tumor growth also causes significant damage to normal tissue. The existing chemotherapy does not give increased survival combined with radiation. For these reasons it is important to further investigate the radiation response in the cells. A greater understanding may contribute to finding new targets for chemotherapeutics, which can hopefully function synergistically with, or at least additive to, radiotherapy. It may also lead to the detection of therapeutic markers that can sort out patients with need for more aggressive therapy.

1.3 Radiation

Radiation of any biological material, such as cells, can lead to excitation or ionization [26]. If the rays hitting the cells carry sufficient energy to briefly elevate an orbiting electron to a higher level in an atom or a molecule, the radiation leads to excitation. If the same electron is hit by radiation carrying a larger amount of energy, the electron will be ejected. The process is then called ionization, and the radiation leading to it ionizing. An example of a source leading to excitation is a laser. X-rays is one type of ionizing

radiation. Radiation energy depends on the length and the frequency of the waves. High frequency and short wavelength represents high energy. One unit describing radiation dose is Gray (Gy). One Gy is defined as the absorption of one joule of radiation energy by one kilogram of matter.

1.3.1 Cellular response to ionizing radiation

Cellular stresses can lead to various types of DNA damage as indicated in figure 4 [11;27]. Ionizing radiation most commonly result in breakage of the phosphodiester bonds in the backbone of the DNA helix. When these breaks are close to each other and on opposite DNA stands, a double strand break (DSB) occurs.

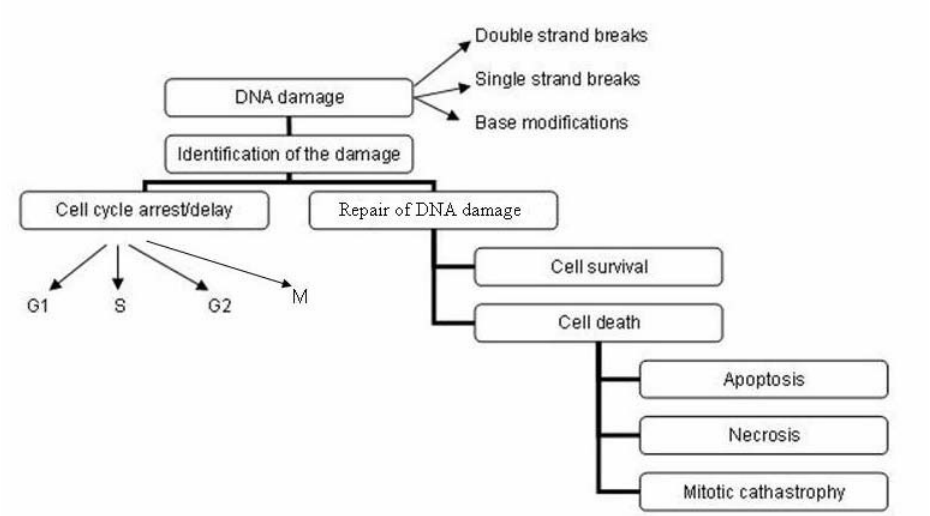

Figure 4. *Possible outcomes of DNA damage due to genotoxic stress such as ionizing radiation.*

In response to DNA damage, a cell activates a machinery to repair it [11;28]. To optimally repair the damage, other cellular processes concerning DNA replication or mitosis must also be regulated. DNA damage can occur in the cell in all phases of the cell cycle, but if it arises in S phase it is particularly challenging because of the ongoing process on DNA replication. Regardless in what phase the DNA damage is caused, the cell greatly benefits from halting or slowing down its progress through the cell cycle until the damage is repaired. If the damage is too severe, cell death is mediated (figure 4).

Some regulators activated after DNA damage caused by ionizing radiation will activate TP53, causing G1- and/or G2 delay or arrest. Both TP53 dependent and independent mechanism are involved in G2 arrest [29]. TP53 is suggested as more important for sustaining the arrest rather than initiating it [11]. Others regulators of cell cycle are activated by a halt in the replication fork machinery as a response to DNA damage in the S phase, leading to a retardation of the cells through this phase [11;28].

G2 arrest after DNA damage is seen also in cells with unfunctional TP53, like HPV 16 or 18 infected cervical carcinoma cells [21;23]. There is still much that is unclear concerning the mechanisms causing arrest after exposure to ionizing radiation. The CKS2 protein may play an important role, but so far this is unknown.

1.4 Basic principles of fluorescence, fluorochromes and antibodies

1.4.1 Fluorochromes and fluorescence

When a fluorescent compound is illuminated with a light source giving the proper radiation, excitation occurs (section 1.3). This happens only briefly; the electron will soon return to its original state, disposing of the excess energy as a photon [30;30;31]. This energetic transition is referred to as fluorescence, and the photons fluorescent light. The emitted fluorescence is always of higher wavelength/lower energy than the light used to excite the fluorochrome. Fluorescent compounds are often referred to as fluorochromes.

The wavelength of the radiation leading to excitation in one fluorochrome is highly specific, as is the wavelength of the photons emitted as fluorescent light from that same compound. Specters showing each fluorochromes specific excitation and emission maximum are available. An example is shown in figure 5.

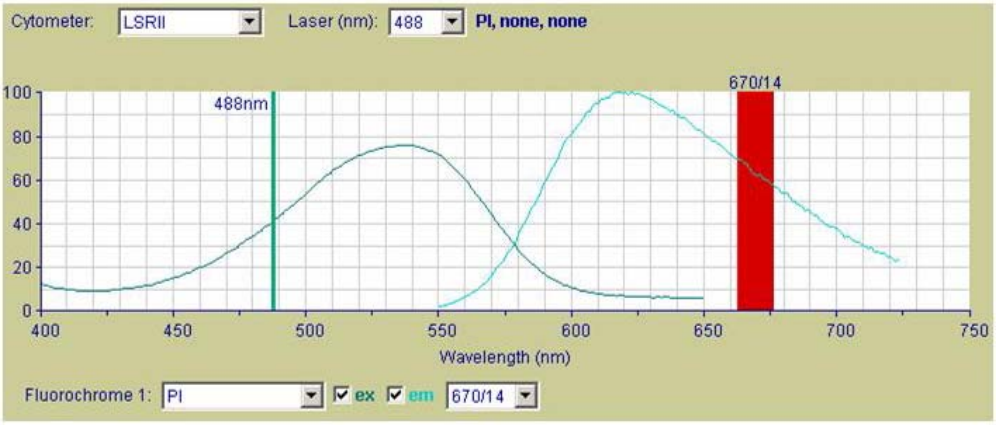

Figure 5. *PI spectra showing ranges of wavelengths for excitation and emission. Laser (green area) and filters used in the LSR II to detect PI (red area) also shown [32].*

Lasers provide light of highly specific wavelengths and are useful radiation sources in generating fluorescence. This gives the possibility of creating and detecting fluorescent light from only one fluorochrome at a time even in the presence of other fluorescent compounds.

1.4.2 Antibodies

Antibodies are proteins which bind with high affinity to specific structures in a corresponding antigen [33]. These structures are called epitopes (figure 6). When an antigen is introduced to a host, production of specific antibodies against that antigen will be initiated in the hosts B-lymphocytes. Antibodies can be commercially produced and used as probes in research for detecting specific proteins. The antibodies are manufactured by activating B-lymphocytes in different hosts. Commonly used hosts are mice, rabbits or goats. If the antibody binds directly to the desired protein it is referred to as a primary antibody (figure 6).

Tissue from other species is also considered as an antigen when introduced to a host. It is therefore also possible to acquire antibodies directed against the host from which the primary antibody was obtained. These antibodies will be referred to as secondary antibodies since they bind to primary ones (figure 6). Fluorochromes can be conjugated

to antibodies (figure 6). Detected fluorescence after illumination of the sample will indicate the presence of the antigen to which the probe binds.

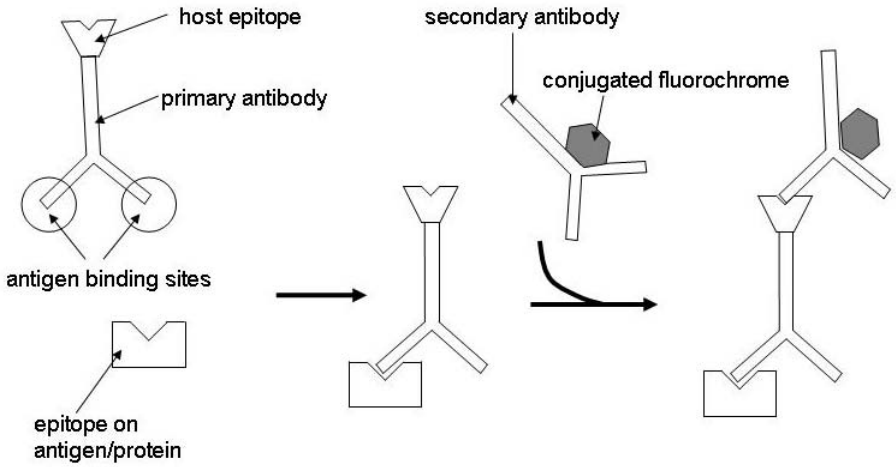

Figure 6. *Primary- and secondary antibodies binding to the target protein/antigen*

The number of epitopes on the antigen determines the maximum number of antibodies that can bind to it. A primary antibody may have several epitopes to which a secondary antibody can bind. Therefore, a higher fluorescent signal can be detected from a sample where secondary antibodies with conjugated fluorochromes were used instead of primary antibodies with conjugated fluorochromes. Secondary antibodies with conjugated fluorochromes can in this way be used to amplify the fluorescent signal when cellular components of low concentrations are being measured. A suitable method for analysing samples dyed with fluorochromes is flow cytometry.

1.5 Flow cytometry

Flow cytometry is used to measure and analyze characteristics of cells (and also other single particles) flowing in fluid stream through a light beam (laser) [30;31]. The laser can be used to specifically create excitation of fluorochromes and detect the corresponding emitted fluorescence. The scatter of the laser beam also gives useful information about the cells in the sample.

The accessibility to a large range of fluorochrome conjugated antibodies and fluorochromes for dying DNA makes flow cytometry a highly suitable method for analysing protein content and cell cycle distribution in cell samples.

Any suspended particle in the size range of 0.2-150 μm in diameter is suitable for flow cytometry analysis[30]. Light scatter is recorded as forward- and side scattered light. Forward scattered light is highly correlated with cell size, while the amount of side scattered light indicates internal granularity or complexity of the cell. The intensity of the emitted fluorescence from a fluorochrome indicates the relative amount of the cellular constituent labelled as described in the previous section. One can also use the flow cytometer for sorting cells according to their measured properties of fluorescence or their light scatter.

Since I have only used the BD LSR II in my experiments, I will focus on describing the functions of this device. The basic principles will be valid for other flow cytometres as well, but there will be slight practical differences.

1.5.1 The LSR II flow cytometer

The flow cytometer consists of three systems:

1. The fluidic
2. The optical
3. The electronical

The fluidic system is the sample's entrance to the instrument [30]. The prepared sample is introduced to the sample injection tube in the sample injection port, and through this the sample will be pressurized upwards into the flow cell by means of a vacuum pump (figure 7). This pump causes the sample fluid stream to enter the flow cell with a slight overpressure compared to the sheath fluid running coaxial on all sides. The difference in pressure restricts the sample stream to the centre of the flow cell, a process which is

called hydrodynamic focusing. Having the cells in a narrow stream in the flow cell, where the cells pass one at a time through the laser beam, gives optimal conditions for illumination by the laser.

The width of the sample stream can be regulated by changing the sample pressure on the control panel. This is shown in figure 7. For analysis where high resolution is needed, ex. in DNA analysis, it is wise to choose a low sample pressure.

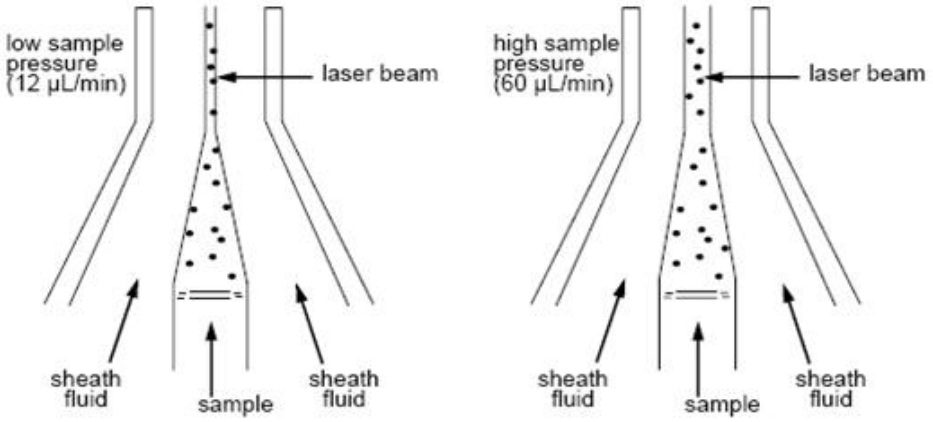

Figure7. *Illustration of cells moving through the flow cell, and changes in the width of the sample stream in response to changes in sample pressure.*

2. The optical system consists of lasers, filters and detectors.
The lasers used and their excitation wavelengths [31]:

- Blue (Coherent Sapphire™), 488 nm (fixed)
- Ultraviolet 325 nm (optional)
- Violet 405 nm (optional)
- Red 633nm (optional)

The lasers illuminate the cells in the sample stream to give the scattered light signals and also excite fluorescent molecules associated with the cells[30;31]. The scattered- and emitted fluorescent light is guided to the appropriate detectors through means of different

filters. This directs the light signals recorded from the sample so that the detectors only measure the light in the wavelength range they are set to process.

The following filters are used:
Long Pass (LP) filters – allows passage of light with wavelengths above the given value, while reflecting that below
Short Pass (SP) filters - allows passage of light with wavelengths below the given value, while reflecting that above
Band Pass (BP) filters – allows passage of light with wavelengths within the given interval, while reflecting that above and below the values.

There are two types of detector arrays in the LSR II [31]:

- The photodiode
- The photomultiplier tubes (PMTs)

To make the PMTs detect faint signals, it is possible to apply voltage to them. This will lead to an amplification of the signal to a level it can be detected. Therefore the PMT's are used to detect the weaker light signals such as fluorescence and SSC, while the photodiode detects the strong FSC signal. Figure 8 shows how the signals arising from illumination of a sample by the lasers is directed to the appropriated detector.

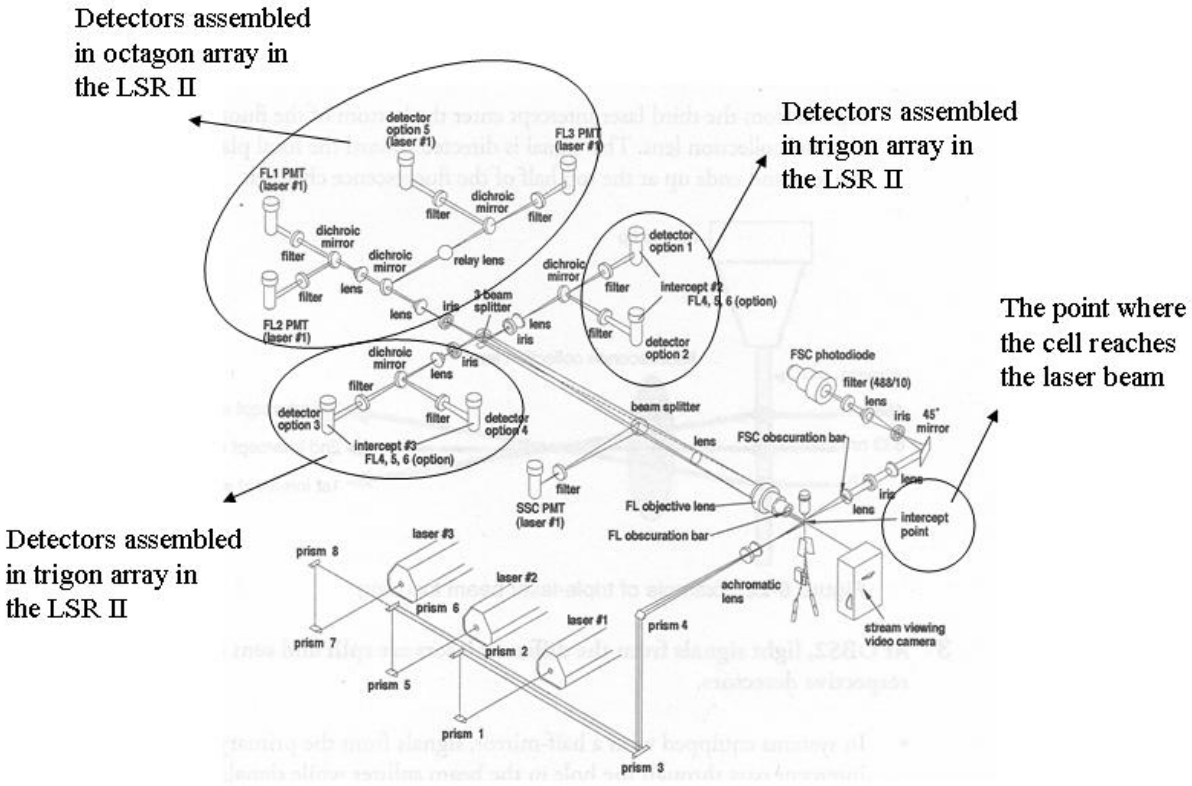

Figure8. *Schematic overview of the light paths in a flow cytometer. Here, a FACSVantage is shown, but the principles are the same in the LSR II. In the FACSVantage the detectors are not gathered in arrays as in the LSR II (figure 9). The LSR II has one more laser with a corresponding trigon detector array. In the LSR II, the SSC PMT is a part of the octagon array. Another difference is the 3 beam splitter which directs the light to their appropriate detectors. In the LSR II, this is exchanged with optical fibers. The filters (mirrors) direct the light beams to their corresponding detector/PMT.*

The signals obtained from illumination of the cells with one laser will be detected by the corresponding PMT array. The detectors for signals arising from illumination by the blue laser are arranged in an octagon (figure 9a). The three other lasers have trigons (figure 9b).

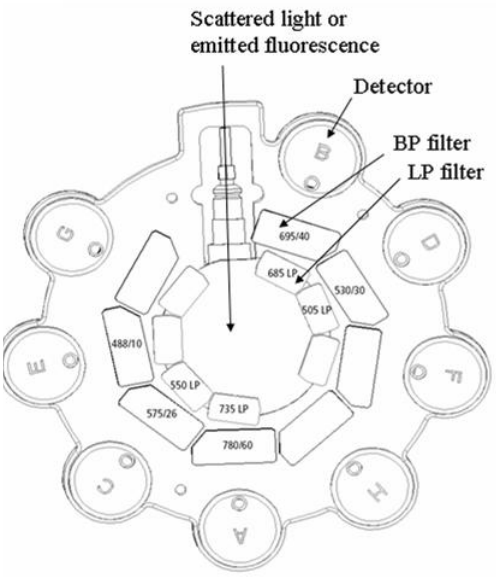

Figure 9a. *The octagon*

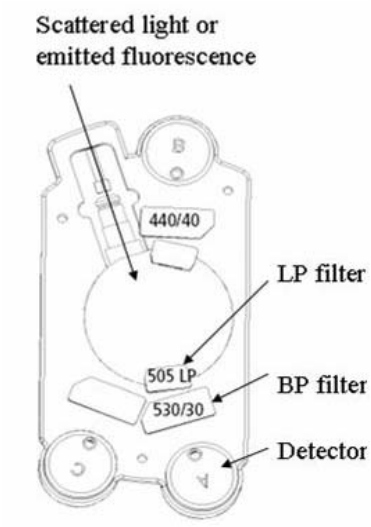

Figure 9b. *The trigon*

The octagon contains eight detectors (a) while the trigon has three (b). In front of each detector there are different filters. The scattered light or emitted fluorescence is introduced to the PMT array at a certain angle, hitting the filters in front of the first detector. If the light is of the wavelength permitting passage through the filters, the light will be admitted through the filters and to the detector behind them. If the light is of another wavelength, it is reflected at such an angle that it is introduced to the next filters, to see if it is allowed to pass through to their corresponding detector and so on [31].

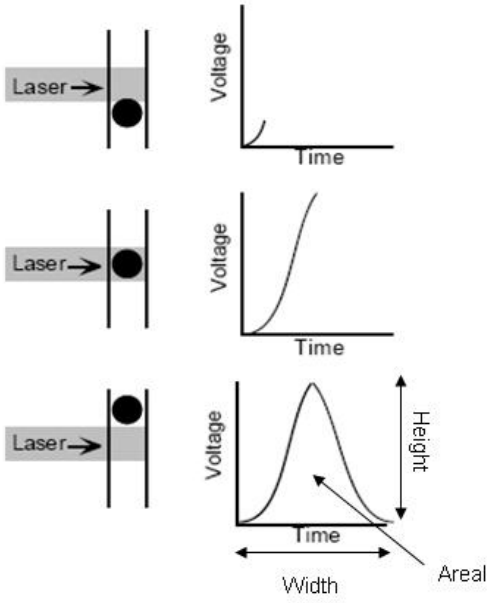

Figure 10. *Converting a cells passage through the laser beam into a pulse [30].*

The detectors will transfer the signal to the electronical system as a pulse for each particle/cell that passes through the laser beam. Each recorded pulse is converted to a digital number, each number correlating to a channel in the range 0-1000 mV. For each pulse, the area, height and width of the curve created is detected (figure 10)

Setting an electronic threshold minimizes or eliminates potential debris detected in the sample. By eliminating noise in this manner, the number of events needed to be detected in the flow cytometer is reduced, since only particles with signal equal to or above the specified threshold value will be detected. Using the software on the computer, data can be stored and analyzed.

1.5.2 Compensation

Sometimes it is beneficial to stain one cell sample with several fluorochromes. It is necessary for measuring DNA, protein(s) and other cellular components in the same sample simultaneously. The used fluorochromes must have a difference in emission maximum wavelength which allows them to be recorded with different detectors (figure 11).

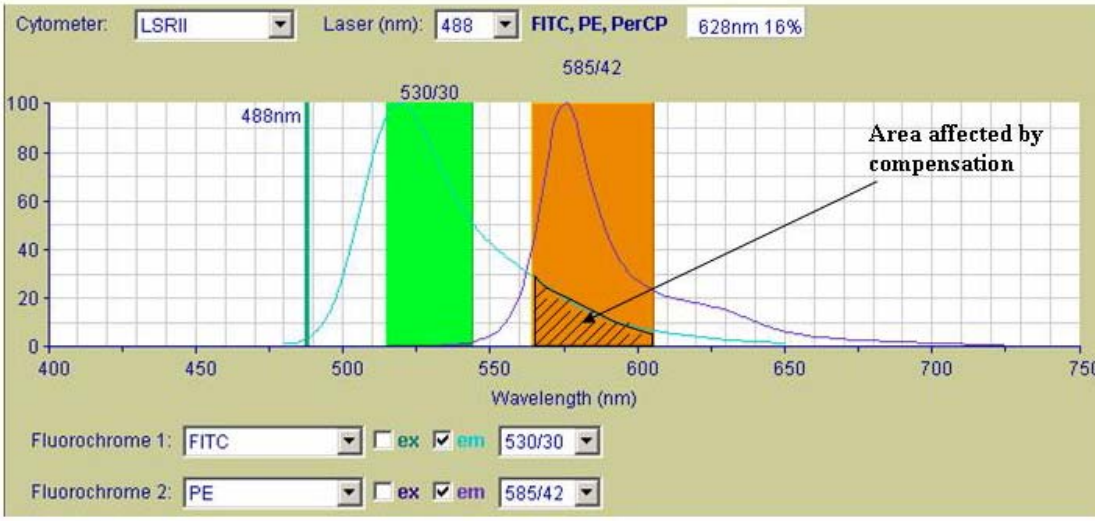

Figure11. *Spectra showing the range of wavelength emitted from FITC (light blue line) and PE (dark blue line) with the overlap indicated as the "area affected by compensation". The laser used to excite the two fluorochromes is shown together with the range of wavelengths applying to the PMTs set to detect the FITC (green area) and PE signals (orange area). There is also a small contribution from PE to the detector set to record the FITC signal, but this is not shown in this figure.*

The emission spectra of different fluorochromes vary in shape, and some can emit light with relatively strong intensity from a great range of wavelengths (figure 5 and 11).

This can lead to overlap of emission spectra as shown in figure 11. The signal from one fluorochrome then appears in a detector used for the other fluorochrome [31]. The quantity of such spectral overlap must be accounted for and the signal intensities must be corrected in the recorded samples. By running calibrating beams it is possible to determine the fluorescent “spill over” as a percentage of the total signal measured in the detector set for the fluorochrome. This percentage is subtracted from the overestimated signal in the other detector. This is called compensation.

METHODS

2.1 The cell lines

The two immortalized cervical epithelial cell lines Hela and Siha were used in the experiments. Hela cells are HPV-18 positive cells obtained from adenocarcinoma, while Siha is HPV-16 positive and originates from squamous cell carcinoma [34;35] They are both established from tissue samples taken from tumors in human cervix. Siha and Hela are two very useful cell lines for research on cervical cancer because of their infection with high risk HPV as well as their origin from the two most common types of cervical cancer.

Both cell lines are adherent and grow as monolayers in culture. Dulbecco's Modified Eagles Medium with added 1% Penicillin Streptomycin, 1 % L-glutamine and 10 % Foetal Bovine Serum was used for culturing. A further description of cell culturing is given in appendix 1-3. Culturing flasks are referred to as T_{25} or T_{75}. The numbers indicate the area in cm^2 in which the cells are cultured. The protocols described were used for both Hela and Siha cells.

For optimal growth Hela cells were splitted when their cell density was about 70-80,000 cells/cm^2 in subcultivating ratios of 1:3 to 1:6. Medium was shifted or added 3 times a week. Siha cells were splitted in subcultivating ratios 1:3 to 1:8 when their cell density was 200,000 cells/cm^2 and medium was shifted or added 2-3 times a week.

2.2 Radiation

Irradiation of cells was done at room temperature with 200 keV X-rays (Siemens, Munich, Germany) which gave a dose rate of 387 rad per minute. A 0.5 mm copper filter was used to provide a homogenous radiation field of a certain area. The area of a T_{25} cultivating flask is within the size of the radiation field. 100 rad equals 1 Gy. The times of exposure to ionizing radiation to give the wanted doses in Gy, were calculated from formula 1.

Formula 1.

387 rad / 60 seconds = 100 rad / x seconds

2.3 Cell experiments

2.3.1 Growth curve

The growth experiment was carried out on Hela and Siha cells as described in appendix 4. It was performed in collaboration with another student. Predetermined numbers of cells from the desired cell line were seeded out into cultivating flasks. Each day, the number of cells in three separate culturing flasks was determined. This gave the opportunity to observe the gradual increase in cell numbers over a period of time. The experiment was completed after 9 days for Hela and 14 days for Siha cells.

By plotting a growth curve from the numbers collected, it was possible to determine the length of the lag phase, at which cell densities the cells had exponential growth as well as maximal cell density. Exponential growth is where the cell number increases by a constant fraction in equal intervals of time [36]. A growth curve also made it possible to determine the time it takes for the cells to complete one full cell cycle and divide. This is called the doubling time (T_d) and was calculated from formula 2.

Formula2.

$\ln (N_{tot} / N_0) = t * \ln 2 / T_d$

The number of cells in each flask was determined by three outtakes. The cells were counted on a colter counter. Figure 12 shows an overview of the daily process for counting the number of cells in three culturing flasks.

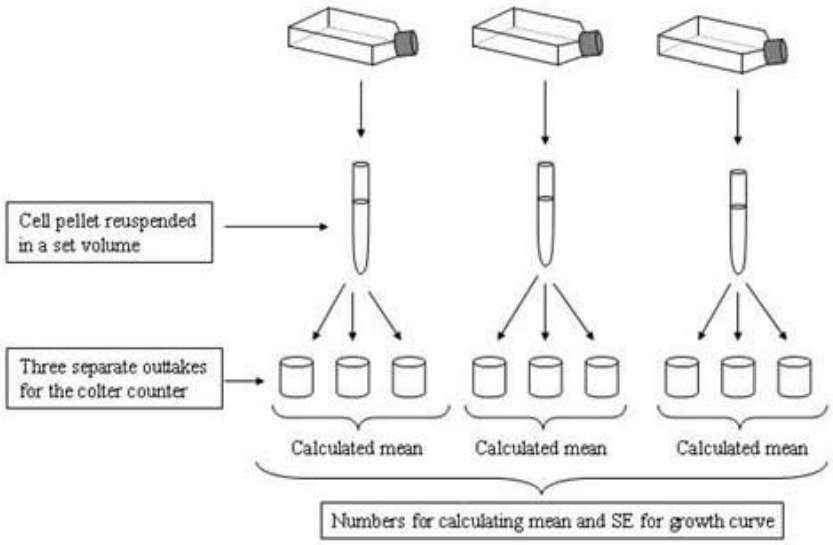

Figure12. *An illustration of how the number of cells in three culturing flasks was counted each day. It also shows what numbers that gave rise to the points and error bars in the growth curve.*

2.3.2 Clonogenic assay

When culturing cells, not all cells seeded out into new cultivating flasks will survive [37]. In the context of clonogenic assay, survival is considered as retaining the ability to divide. Performing a clonogenic assay is therefore one way of illustrating a cell line's average ability of resistance to the factors involved when handled in the laboratory.

The experiment was carried out as described in appendix 5. It was performed in collaboration with another student. Predetermined numbers of cells (table 2) were seeded into cultivation flasks and left in the incubator for 17 days. The formed colonies were fixed and dyed as described in appendix 6.Colonies containing 50 cells or more were considered proof of intact reproductive integrity of an initially seeded cell. These macroscopic colonies were counted under a magnifying glass. The percentage of cells seeded that grow into colonies is known as the plating efficiency (PE). PE was calculated from formula 3 [37].

Formula 3.

PE = (Number of colonies counted / Number of cells seeded) * 100

Table 2. *Number of cells seeded out for both Hela and Siha cell lines for determining PE in the clonogenic assay.*

50	100	200	400	600	800	1000

2.3.3 Radiosensitivity (Dose response curve)

Radiosensitivity is a cell's susceptibility to the harmful effect of ionizing radiation. A dose response curve illustrates the relationship between radiation dose and the proportion of cells that survive the radiation, the survival fraction (SF) [37].

The experiment was carried out as described in appendix 5. It was performed in collaboration with another student. Predetermined numbers of cells were seeded into culturing flasks and left in the incubator for 24 hours. The flasks were then irradiated with different doses. All flasks were returned to the incubator and left for 17 days. The colonies formed was fixed and dyed as described in appendix 6. Predetermined cell numbers with corresponding radiation doses are shown in table 3. The SF for each radiation dose was calculated according to formula 4 [37].

Table 3. *The chosen cell numbers and corresponding radiation doses for the different cell lines*

Radiation dose (Gy)	0	1	2	4	6	8	10
Cell no. Hela	300	400	600	1000	5000	30 000	100 000
Cell no. Siha	300	400	600	1000	3000	9000	30 000

Formula 4.

SF = (Number of colonies counted / Number of cells seeded) * (PE / 100)

2.3.4 Harvesting and fixation of cells for flow cytometer analysis

Cells were harvested as described in appendix 7. All medium and trypsin was collected with the cells detached from the culturing flask after trypsin treatment. This was done to make sure that all cells in the culturing flask, including those that had (partially) detached from the culturing surface before trypsin was added, were included in the experiment. The cells were then fixed (appendix 8).

The fixation of cells kills and preserves them in their phase of the cell cycle phase. Most cellular content is also kept at the levels it was when the cell was fixed. The two ways used for fixating cells are described in appendix 8 and were:

- Methanol fixation
- LFM fixation

Methanol fixation involved adding a small volume of methanol to a cell pellet and resuspending the cells. In addition to killing and preserving the cell, the methanol removed fat components in the cell membrane and made it permeable.

The other way of fixating cells was by resuspending the cells in a detergent buffer (appendix 9) before formaldehyde was added [38;39]. The detergent buffer gently lysed the cells, making a nuclear suspension. The formaldehyde fixed the contents of the nuclear suspension. This procedure changes chromatin structure in the cells. This allows separation of cells in G2 and M phase with flow cytometry after staining cell samples with two fluorochromes that bind to DNA in different ways. The way PI and Hoechst 33258 bind to DNA is described in appendix 13. Detergent buffer and formaldehyde was removed and methanol was added to give comparable conditions in all samples where CKS2 protein content was to be measured.

2.3.5 Effects on the cells 24 hours after different radiation doses

The experiment was carried out as described in appendix 10. Cell numbers, dependent on cell survival at the different doses, were seeded out into 12 cultivating flasks. After 24 hours the cells were irradiated with different doses. Two cultivating flasks were exposed to the same amount of radiation. Cells in two of the cultivating flasks were not irradiated, but were otherwise treated similarly. 24 hours after irradiation, the cells were harvested and fixed (appendix 7). The cells being exposed to the same radiation dose were collected in the same tube. The samples were stored at -20ºC and stained and analyzed by flow cytometry later. Figure 13 shows a schematic overview of the steps described above.

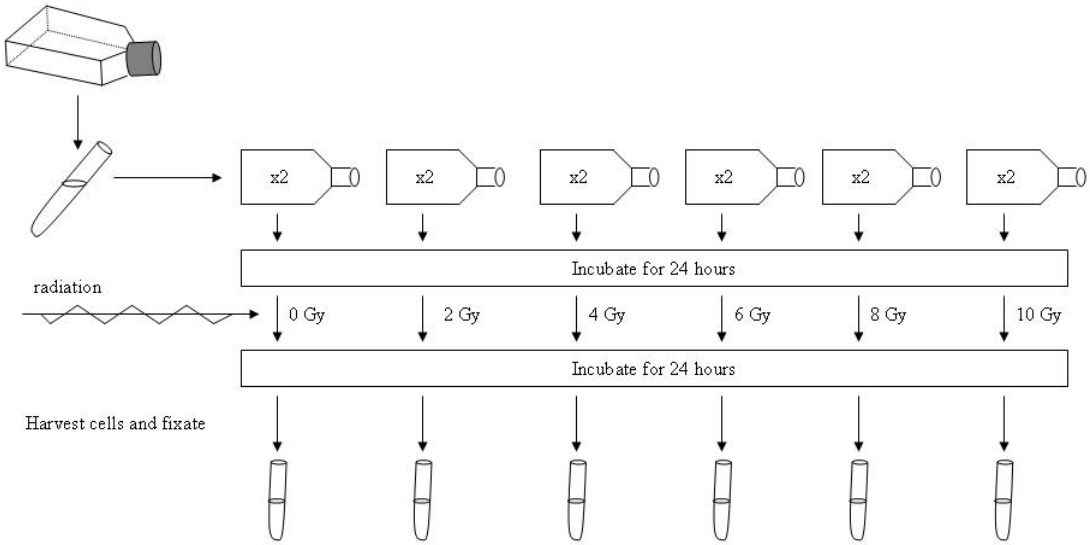

Figure 13. *A schematic illustration of the experimental setup concerning cells harvested and fixed 24 hours after exposure to different radiation doses.*

2.3.6 Effects on the cells different times after irradiation with 8 Gy

The experiment was carried out as described in appendix 10.Cells were seeded into 16 cultivating flasks and left in the incubator for 24 hours. The cells were then irradiated with 8 Gy. Cells in two of the cultivating flasks were not irradiated, but were otherwise treated similarly to the rest of the samples. After different time intervals, two flasks containing irradiated cells were harvested and fixed in the same tube (appendix 7). The flasks containing the non-irradiated cells were harvested and fixed at the same time as the first irradiated sample. The steps described above are summarized in figure 14. Figure 14 also gives the time intervals for harvesting and fixating the cells. The cells were stored at -20ºC and stained for flow cytometry analysis later.

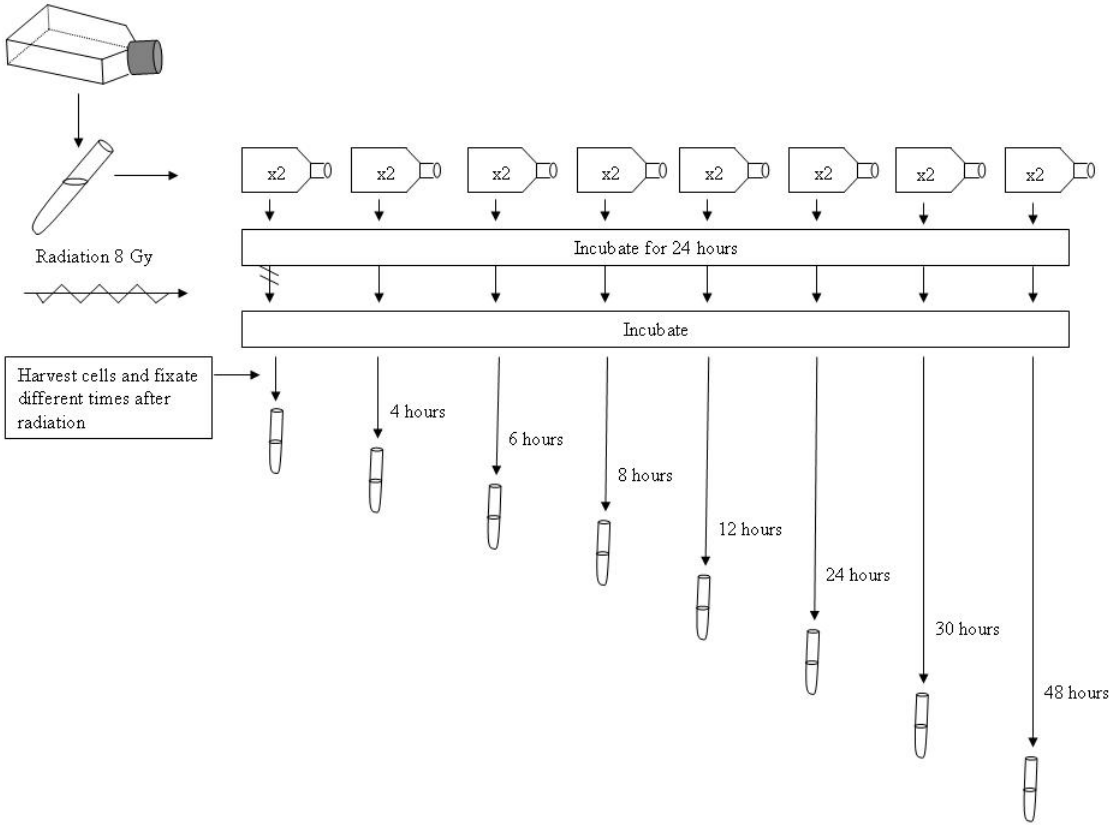

Figure 14. *A schematic illustration of the experimental setup concerning cells harvested different times after being irradiated with 8 Gy. The two flasks containing control cells were not exposed to radiation as indicated.*

2.4 Preparing samples for flow cytometry analysis

The procedure used to stain the cell sample for flow cytometry analysis is described in appendix 11. The final concentrations of all reagents used are listed in table A1 in appendix 11.

All samples were dyed with a primary antibody directed against the CKS2 protein. A secondary antibody with conjugated FITC fluorochrome which binds to this primary antibody was also added to the sample. The content of CKS2 was therefore corresponding to the FITC signal detected in the flow cytometry analysis. The different phases of the cell cycle were separated on the basis of DNA content. The fluorochrome used for this purpose was Hoechst 33258. The cells in G2 and M phase have the same DNA content and needed further separation. In the methanol fixed cells this was done by adding a mitosis marker; anti-PH3. A secondary antibody with conjugated PE fluorochrome which binds to the mitosis marker was also added to the sample (appendix 11, table A2). To separate G2 and M phase cells in LFM fixed cell samples, a second fluorochrome for staining DNA, PI, was added (appendix 11, table A3). In LFM fixed cells, the intensity of the signals from PI and Hoechst 33258 will be different.

The preliminary work to establish this method included a gradual increase in the number of fluorochromes and antibodies added to the cell samples. This ruled out the possibility of interference between the different reagents that could potentially have influenced the results. This also proved the CKS2 antibody staining as a suitable method for detecting the protein content.

2.5 Running samples and processing data with the LSR II

All cell samples were analyzed on a LSR II flow cytometer (Becton Dickinson, Erembodegem, Belgium.) A detailed description of the flow cytometry analysis and the processing of data are found in appendix 12.

The parameters were set so the emission from the different fluorochromes were detected in separate detectors. A threshold was set to eliminate debris. The voltages over the PMTs were set at ranges that included the entire cell population for analysis and recording. The compensation needed for the PE and FITC signal was calculated at the beginning of each experiment. The G1, S and G2-M phases were separated based on DNA content as illustrated in figure 15. The DNA content is represented by the Hoechst 33258 signal as shown in figure B in appendix 12. The G2 and M phase were further separated based on the PI signal illustrated in figure C in appendix 12, or based on the mitosis marker represented by the PE signal shown in figure D in appendix 12. Which method used depended on cell fixation. The CKS2 protein content was quantified in the different phases of the cell cycle based on the CKS2 antibody, represented by the FITC signal shown in figure E1-E4 in appendix 12.

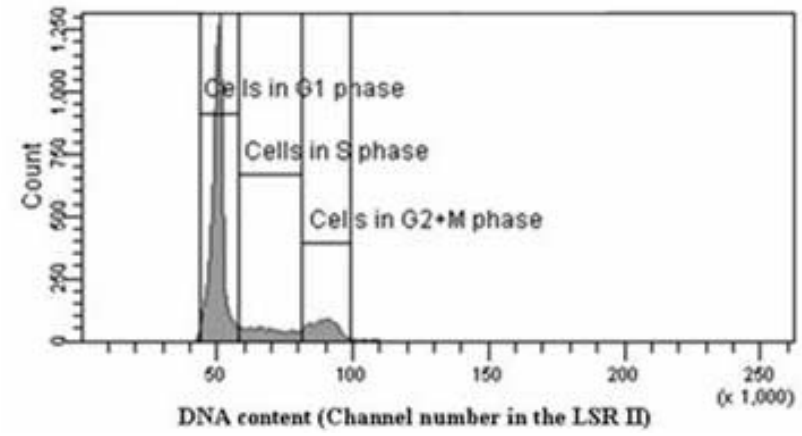

Figure15. *A DNA histogram showing the cell cycle distribution in non-irradiated Hela cells. The separation of the phases G1, S and G2-M is shown. Further separation of G2-M phase and analysis of data are described in the text and in appendix 12.*

For each sample, 10,000 events/cells through the laser beam were recorded. The fraction of cells in each cell cycle was determined by analyzing DNA histograms in the Modfit cell cycle program (Verity Software House, Inc, Topsham, ME.)

To account for variations in the detected CKS2 protein signal between experiments, the numbers obtained regarding relative CKS2 protein content were normalized in each experiment. The protein content detected in G1 in non-irradiated cells was set to the value of 1, and all numbers in the same experiment were given according to this fixed value.

Unspecific binding of FITC conjugated secondary antibody was subtracted from the FITC signal used in results presented in the coming sections. This gives the most realistic measurements of actual CKS2 protein content in each sample.

RESULTS

3.1 Cell line characteristics

3.1.1 Growth curve

The curves in figure 16 illustrate the growth rates of the two cell lines. An initial lag phase was observed for both cell lines. This lasted three days before exponential growth occurred. Hela cells reached the confluent phase at day 5. No further increase in Hela cell number was detected and the experiment was terminated at day 9. The cell numbers detected for the Siha cells at day 7 and 8 did not show the same increase as previously, although cell proliferation continued. At day 14 there was no further growth, and even a declining phase was observed. The experiment was terminated at day 14 for the Siha cells.

The cell numbers obtained from the phases of exponential growth were used to calculate the doubling time for both cell lines (formula 2). The doubling time for the Hela cells were calculated from the increase in cell numbers between day 2 and 5. The curve for the Siha cells is was at its steepest between day 2 and 7, so the doubling time was calculated from the increase in cell numbers counted these days. The calculated doubling time for Hela was 0.9 (~22 hours), while it was 1.4 (~34 hours) for Siha. This showed that the Hela cells multiplied faster than Siha.

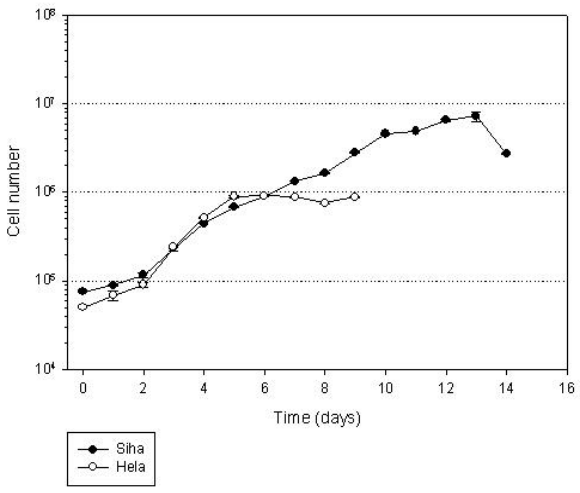

Figure16. *Counted cell numbers of Hela and Siha cells as a function of time. Each point in the curve is a result of the mean value of three parallel samples. The cell number of each sample was determined by three separate outtakes. Bars representing SE are drawn.*

The two cell lines differed with respects to how they respond to a crowded environment and at which cell densities they were able to grow at. When the Hela cells had reached their maximum confluency level, single cells detached from the surface and were seen floating in the medium. The cells that still adhered to the flask surface looked viable. If the medium had been replaced or if fresh medium had been added, these cells would probably have continued dividing and once again created a monolayer of maximum confluency. Still, since medium was neither replaced nor added, all the cells eventually loosened from the surface and died.

The Siha cells on the other hand were able to grow at higher cell densities than the Hela cells, but when they reached confluent phase they collectively loosened from the surface. In the microscope the day after they did not look viable, and none remained attached to the surface of the flask.

Hela cells growing at different cell densities are shown in figure 17. At low confluency they were seen broadly stretching on a relatively large space. Their shape was to a large extent maintained also when the surrounding space became more and more occupied by other cells.

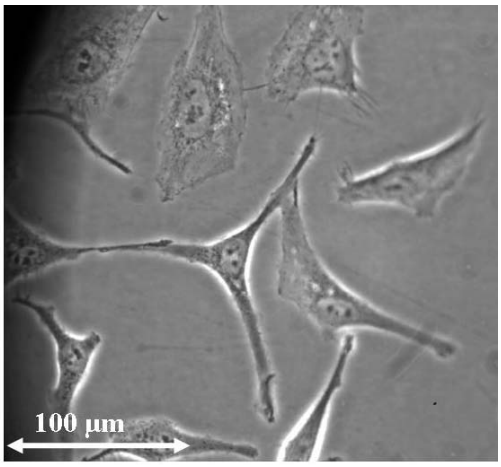

Figure 17a.

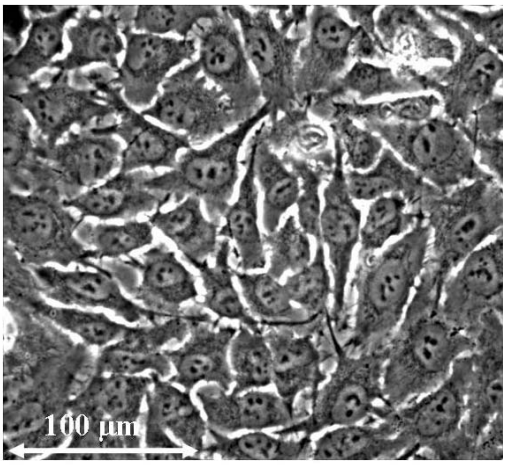

b.

Hela cells growing at low (a) and high (b) cell densities.

Siha cells growing at different cell densities are shown in figure 18. At low cell density, the differences in morphology compared to the Hela cells were minor. The Siha cells stretched slightly more than the Hela cells. At high cell density, Siha cells changed shape and rounded up to small circular units. Consistent with the results from the growth curve, this allowed the Siha cells to grow at higher cell densities.

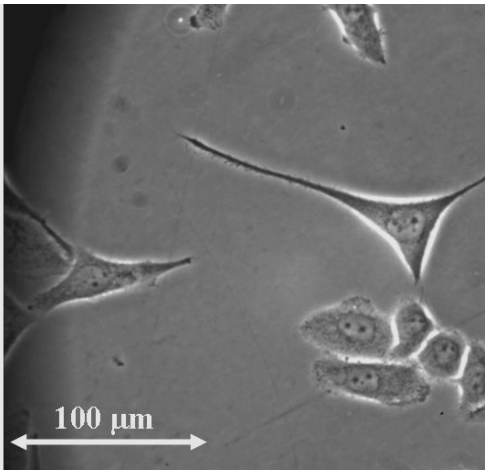

Figure 18a.

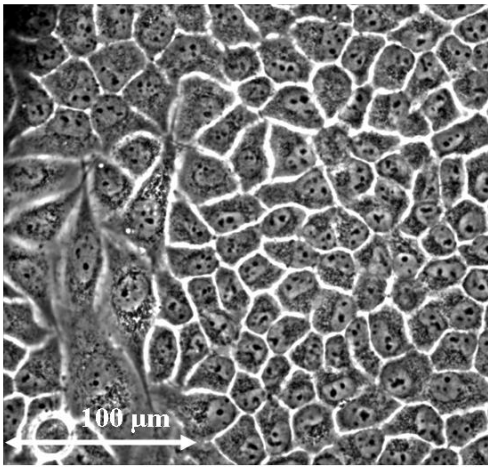

b.

Siha cells growing at low (a) and high (b) cell density.

3.1.2 Clonogenic assay

Table 4 shows the results of the clonogenic assay.

Table 4. *Number of cells seeded and the colonies counted 17 days later for Hela (a) and Siha (b) cells.*

Number of cells seeded		50	100	200	400	600	800	1000
Colonies counted Hela	Parallel 1	36	64	134	160	224	294	364
	Parallel 2	32	57	110	182	224	296	361
	Parallel 3	24	68	120	179	227	311	372
	Mean	31	63	121	174	225	300	366

a.

Number of cells seeded		50	100	200	400	600	800	1000
Colonies counted Siha	Parallel 1	18	47	85	184	260	448	459
	Parallel 2	11	53	93	175	304	395	471
	Parallel 3	19	48	91	168	301	423	466
	Mean	16	49	90	176	288	422	465

b.

PE was calculated from formula 3. PE for Hela was 49±5 (SE) and for Siha 45±3 (SE). There is no difference in PE for the two cell lines.

3.1.3 Radiosensitivity (Dose response curve)

The dose response curve is shown in figure 19. The survival fractions on the y-axis were calculated from formula 4.

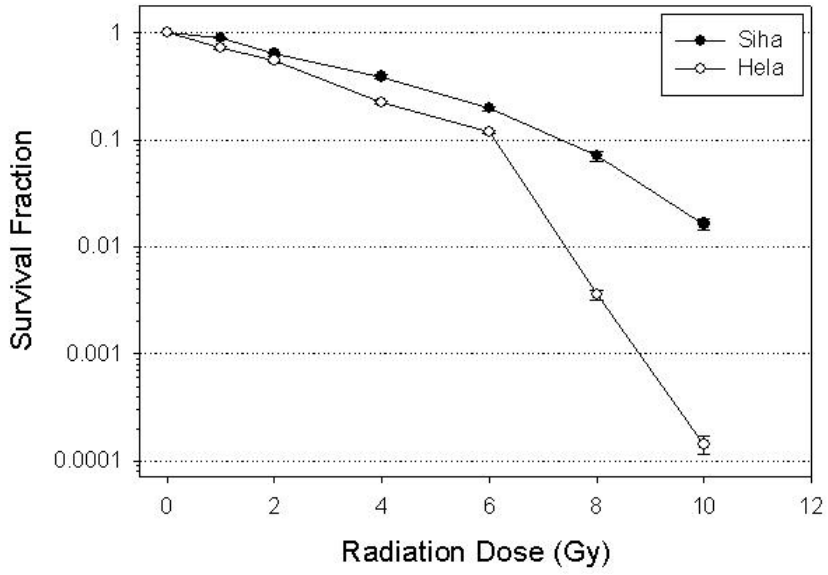

Figure 19. *Surviving fraction as a function of radiation dose with graphs shown for both cell lines. Each point represents the mean of three parallel samples. Bars represent standard error.*

A difference in radiosensitivity between the two cell lines was detected already after 1 Gy. The survival fraction was higher for siha than for Hela (p=0.001). At 2 Gy, the

survival fraction for Siha and Hela cells were not significantly different (p=0.067). At all doses higher than 2 Gy doses, Siha had a significantly higher survival fraction that Hela ($p \leq 0.002$).

These results showed that the Siha cells were more resistant to ionizing radiation compared to the Hela cells, even at low doses.

3.2 Effects of radiation on cell cycle distribution and CKS2 protein content

3.2.1 Changes in cell cycle distribution 24 hours after different radiation doses

As seen in figure 20, there were an increasing number of cells in G2 and a corresponding reduction in G1 with increasing radiation dose. The accumulation of cells in G2 phase was most evident at doses $\geq$6Gy. The number of cells in S phase seemed unchanged.

Figure 21 shows the fraction of Hela cells in each phase of the cell cycle after radiation. The numbers were collected from Modfit analysis of DNA histograms, from which one representative parallel is shown in figure 20.

Figure 21 shows a decrease of cell fraction for the G1 phase in Hela cells with increasing radiation dose. This decrease was first significant at 6 Gy (p=0.028). The cell fraction continued to decrease with increasing radiation dose. A corresponding increase in G2-M phase cell fraction was observed. This increase was significant at 4 Gy (p=0.008), and continued with increasing radiation dose. The fraction of cells in S phase was never significantly different from that detected in the control cells.

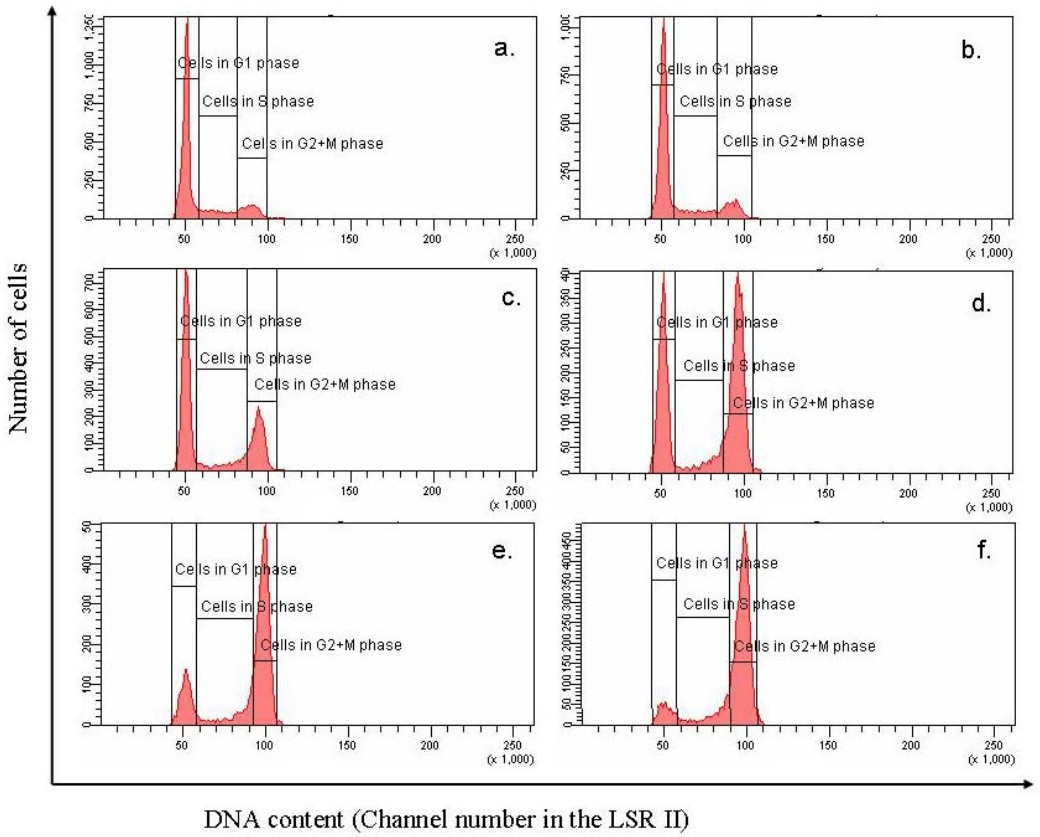

Figure 20. *DNA histograms showing the distribution of Hela cells in the different phases of the cell cycle after exposure to radiation doses of 0(a), 2(b), 4(c), 6(d), 8(e) and 10 Gy (f).The phases G1, S and G2+M are marked in the histograms .The histograms shown are representative for the three separate experiments.*

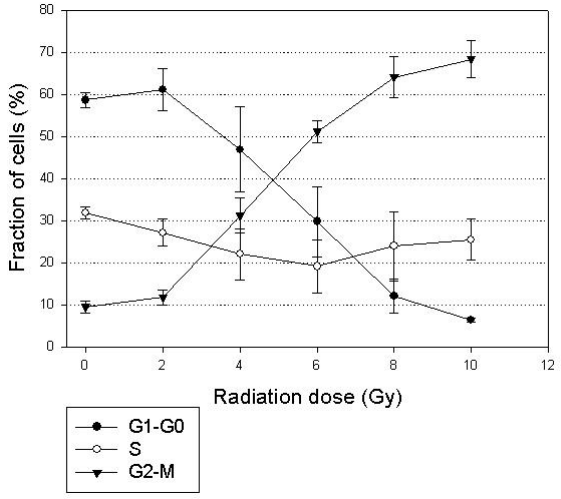

Figure 21. *Fraction of Hela cells in the different phases of the cell cycle as a function of radiation dose. Each point is the mean of three separate experiments. Bars represent standard errors.*

Figure 22 shows the cell cycle distribution in Siha cells in response to radiation with different doses. As for the Hela cells, radiation doses ≥6 Gy gave the largest increase in G2 cell fraction.

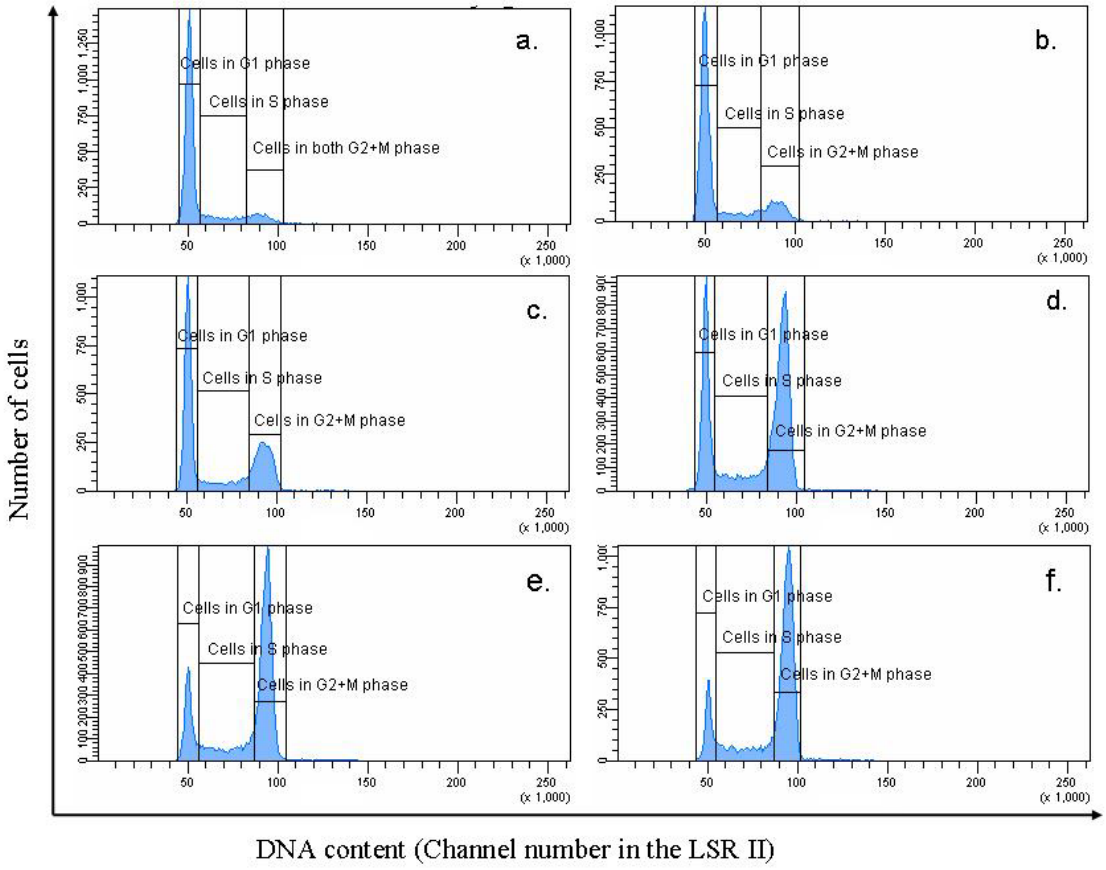

Figure 22. *DNA histograms showing the distribution of Siha cells in the different phases of the cell cycle after exposure to radiation doses of 0(a), 2(b), 4(c), 6(d), 8(e) and 10 Gy (f). The phases G1, S and G2+M are marked in the histograms .The histograms shown are representative for the three separate experiments.*

Figure 23 shows the fraction of Siha cells in the different phases of the cell cycle after radiation. The numbers are obtained from Modfit analysis of DNA histograms, from which one representative parallel is shown in figure 22.

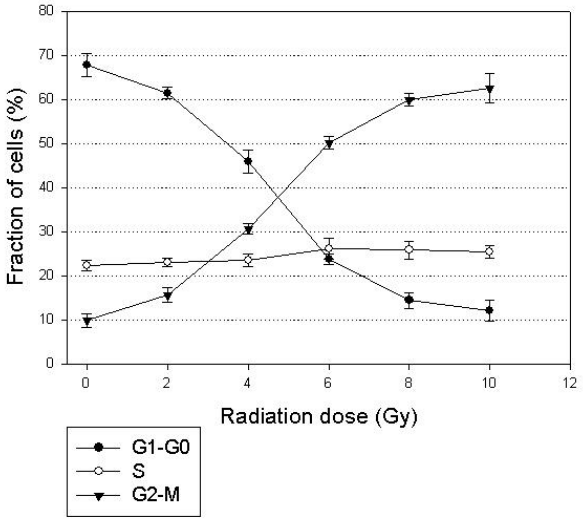

Figure 23. *Fraction of Siha cells in the different phases of the cell cycle as a function of radiation dose. Each point is the mean of three separate experiments. Bars represent standard errors.*

Figure 23 shows a decreasing cell fraction in G1 phase in Siha cells with increasing radiation doses. This decrease was first detected as significant after 4 Gy ($p=0.004$). The decrease continued with increasing radiation doses. An increasing G2-M cell fraction was first detected in the samples being radiated with 4 Gy ($p=<0.001$). There was a further significant decrease with higher radiation doses. There were no significant changes in S phase cell numbers in response to radiation.

The effects on cell cycle distribution in response to ionizing radiation were the same for the two cell lines. The increasing fraction of cells in G2-M may be due to an arrest. This possible G2 arrest seemed to affect an increasing number of cells with increasing radiation dose.

Comparing the cell distribution in the non-irradiated Hela and Siha cells, there were slight differences. There were more cells in the S phase for Hela cells (32% ± 1 %) than for Siha (22% ± 1 %). Moreover, the fraction of cells in G1 phase was lower for Hela (59% ± 2 %) compared to Siha (68% ± 3 %), whereas the percentage of the cells in G2+M phase was similar (9-10% ± 1-2 % for Hela and Siha respectively). This means that a larger percentage of Hela cells were moving through the cell cycle compared to Siha cells. This is in agreement with the observed higher growth rate for Hela compared to Siha.

3.2.2 CKS2 protein content 24 hours after different radiation doses

Figure 24 shows CKS2 protein content measured in Hela cells with the LSR II. Each phase of the cell cycle is shown separately.

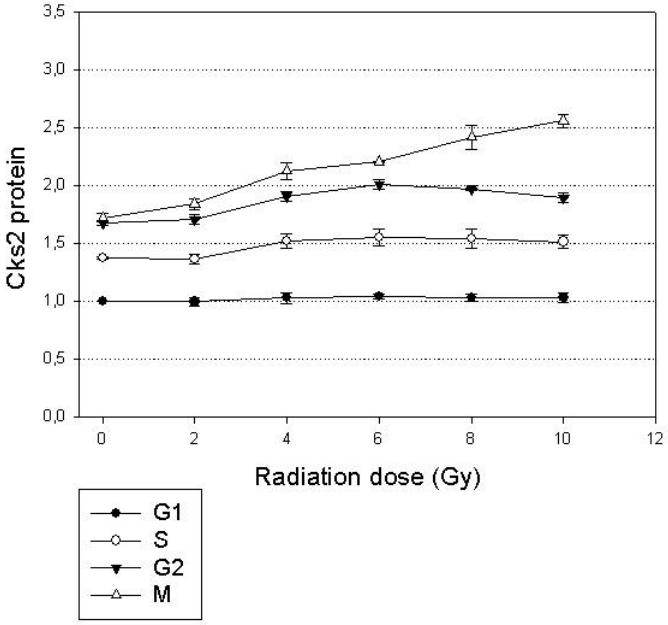

Figure 24. *Graphs showing CKS2 protein in different phases of the cell cycle in Hela cells as a function of radiation dose. The protein content is measured in cells fixed in methanol 24 hours after radiation. Each point is the mean of three separate experiments. The bars represent standard error.*

The CKS2 protein in G1 and S phase was not affected by radiation. There was an increase in CKS2 protein content in G2 phase after the radiation dose of 4 Gy ($p=0.007$). There was no further increase with increasing radiation doses. The CKS2 protein content in the M phase cells increased with increasing radiation doses. This was first detected after 4 Gy ($p=0.009$) and continued to increase significantly with increasing radiation dose. At 10 Gy, the CKS2 protein content in M phase was 49 % ± 6 % higher compared to the same phase in control cells.

Figure 25 illustrates the CKS2 protein content in the different parts of the cell cycle Siha cells in response to radiation.

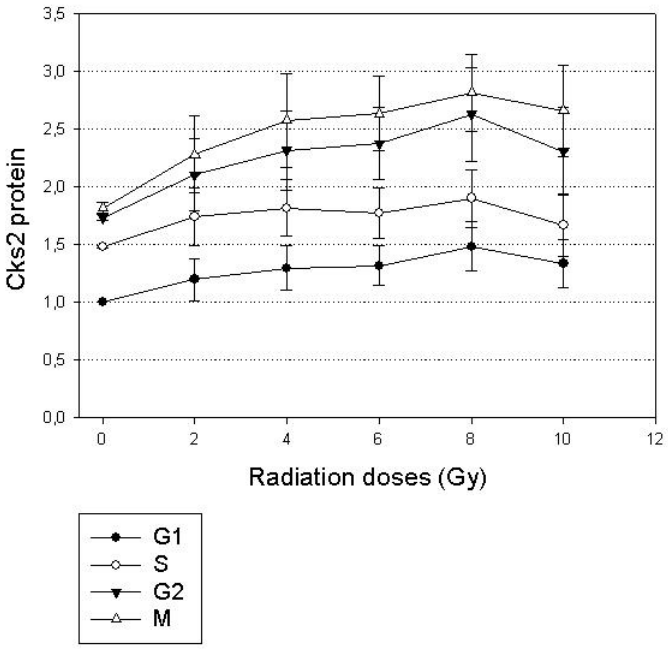

Figure 25. *Graphs showing CKS2 protein in different phases of the cell cycle in Siha cells as a function of radiation dose. The protein content is measured in cells fixed in methanol 24 hours after radiation. Each point is the mean of three separate experiments. The bars represent standard error.*

The changes in CKS2 protein content in the phases G1, S and G2 in response to radiation were not significant in these experiments.

In M phase, an increase in CKS2 protein content is detected after radiation with 8 Gy ($p=0.041$). At 10 Gy, there was no further increase in measured protein content ($p=0.781$) compared to the levels at 8 Gy. Still, at 10 Gy there was a 46 % ±21 % increase in CKS2 protein content in M phase compared to M phase in control cells.

An increased level of CKS2 protein in M phase is seen with increasing radiation doses for both cell lines. In Hela cells, an increase in CKS2 protein content in G2 cells was also observed. An increase in protein levels was not seen for the other phases.

Comparing the distribution of CKS2 protein content in the different phases of the cell cycle in non-irradiated control cells, the levels detected in G1 phase is significantly different from all other phases. The same applies to S phase. The measured content of CKS2 protein content in methanol fixed cells show equal levels in G2 and M phase ($p=0.326$ for Hela and $p=0.170$ for Siha). These levels are higher than those detected cells in both G1 and S phase.

3.2.3 Changes in the cell cycle distribution different times after irradiation with 8 Gy

Figure 26 show the development over time on the distribution of Hela cells in the different phases of the cell cycle after radiation with 8 Gy.

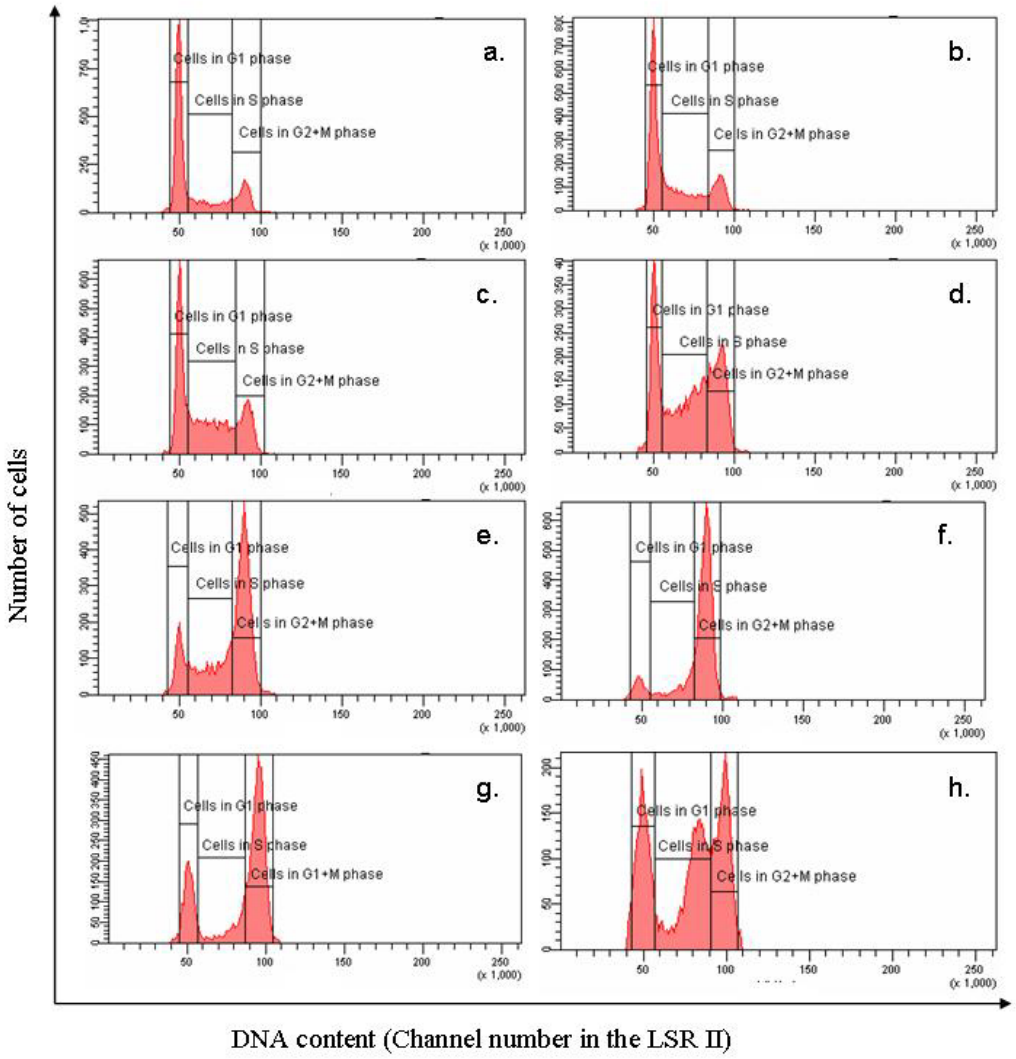

Figure 26.*DNA histograms illustrating the cell cycle distribution in Hela cells 4(b), 6(c), 8(d), 12(e), 24(f), 30(g) and 48(h) hours after radiation with 8 Gy. Non-irradiated cells are shown in a. The phases G1, S and G2+M are marked in the histograms. The histograms are representative for the three separate experiments.*

An increase in the number of cells was seen in S phase after 6 hours. At 24 hours, the cells that moved slowly from G1 through S phase had accumulated in G2-M phase. After

30 hours, there were an increasing number of cells in G1. After 48 hours a peak of cells in S phase was forming between approximately equal numbers of cells in G1 and G2 phase.

Figure 27 shows cell fractions of Hela cells in the different parts of the cell cycle different times after radiation. The numbers are collected from Modfit analysis of DNA histograms, of which one representative parallel is shown in figure 26.

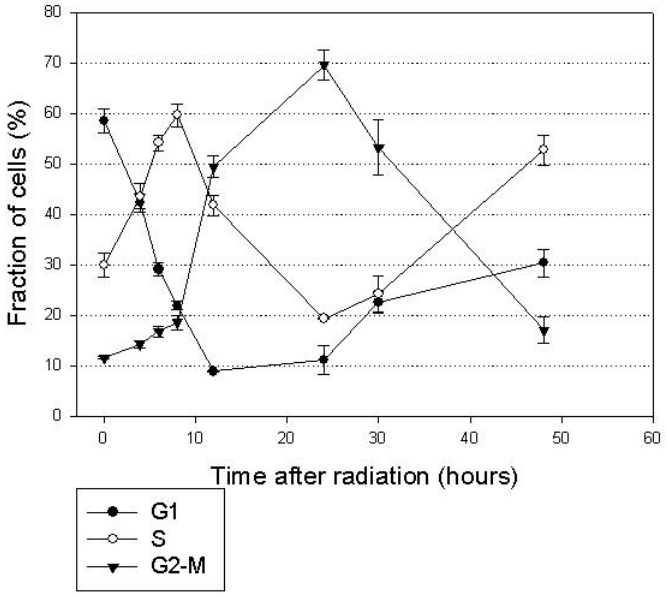

Figure 27. *Fraction of Hela cells in different phases of the cell cycle as a function of time after radiation with 8 Gy. Each point is the mean of three separate experiments. Bars represent standard error.*

Figure 27 shows a decrease in the fraction of cells in G1 phase. This is detected after 4 hours (p=0.005), and continues to a minimum 12-24 hours after radiation. The fraction of cells in G1 increased between 24 and 48 hours (p=0.009), but to a number significantly lower than for non-irradiated cells.

An increase in fraction of cells for S phase was seen after 4 hours (p=0.016). This increase gradually continued to a maximum after 12 hours. The levels then decreased to a minimum 24 hours after radiation (p=<0.001), before a second increase was seen at 48 hours (p=<0.001). This increase at 48 hours did not reach the same levels as that detected at the maximum at 8 hours (p=0.040).

Also for cells in G2-M phase, an increase in cell fraction was seen after 4 hours (p=0.027). This increase continued and reached a maximum after 24 hours. A decrease from the levels at 24 hours was seen after 48 hours (p=<0.001). After 48 hours, the level of cells detected in the G2-M phase was actually no different from that in the control cells (p=0.114).

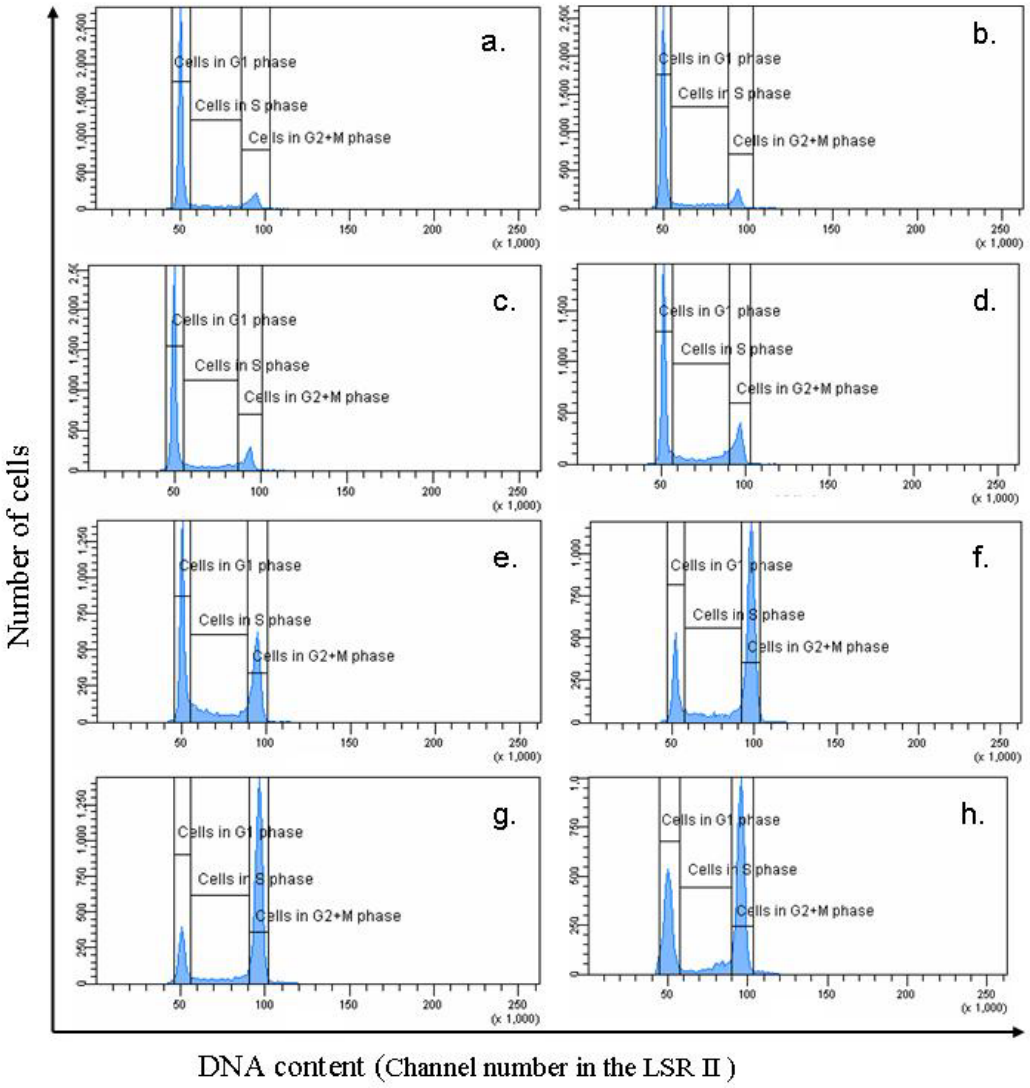

Figure 28. *DNA histograms illustrating the cell cycle distribution in Siha cells 4(b), 6(c), 8(d), 12(e), 24(f), 30(g) and 48(h) hours after radiation with 8 Gy. Non-irradiated cells are shown in a. The phases G1, S and G2+M are marked in the histograms. The histograms are representative for the three separate experiments.*

Figure 28 show DNA histograms of Siha cells different times after radiation with 8 Gy. Compared to the Hela cells, the amount of cells in S phase appeared to be less affected by the radiation. Cells from G1 seemed to move through S phase and accumulate in G2, reaching a maximum level after 30 hours. Cells may have entered M phase and subsequently G1 phase after 48 hours, since an increased cell number in observed for G1.

Figure 29 shows the fraction of Siha cells in the different parts of the cell cycle different times after radiation. Numbers are collected from Modfit analysis of DNA histograms obtained by flow cytometry. DNA histograms from one representative parallel are shown in figure 28.

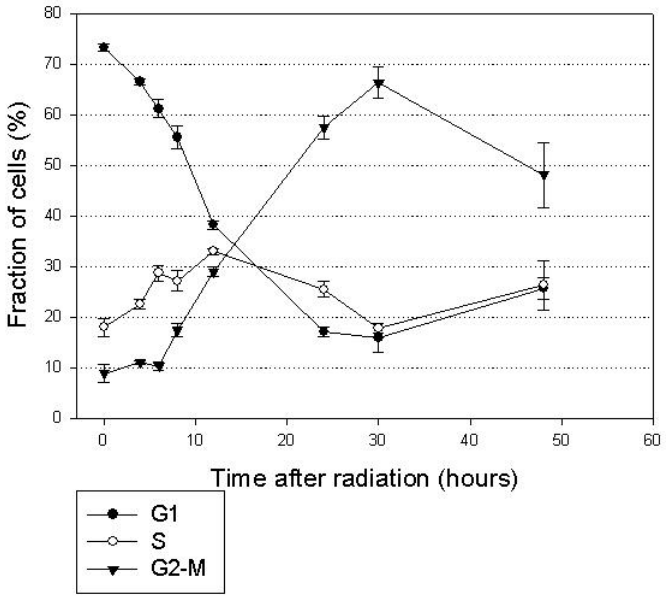

Figure 29. *Graphs illustrating the changes in cell cycle distribution in Siha cells different times after exposure to the radiation dose 8 Gy. Each point is the mean of three separate experiments. The bars represent standard error.*

Figure 29 shows some of the same trends in Siha cells as figure 27 did for Hela cells; a rapid and significant increase in the fraction of cells in S and G2-M phase and a decrease in G1, all of which are gradually returned towards normal at later times after reaching a maximum. The decrease in fraction of cells in G1 was detected as significant after 4 hours ($p=0.002$) and reached a minimum after 24 hours. The cell fraction in S and G2-M was increased after 6 ($p=0.010$) and 8 hours ($p=0.019$), respectively. The fraction of cells

in S phase reached a maximum after 12 hours, while it for the G2-M cell fraction was after 30 hours.
The first increase in the fraction of cells was considered the result of retardation through S phase in response to DNA damage inflicted by the ionizing radiation. The accumulation of cells in G2-M phase is possibly the result of a G2 arrest previously mentioned (section 3.2.2). The cells in both cell lines seemed to initiate the G2 arrest immediately after radiation. After 24-30 hours, this G2 arrest seemed to be abolished and the cells gradually continued through the cell cycle.

The distribution of cells in S phase different times after radiation show comparable patterns in both Siha and Hela cells, although the actual fractions of cells differ. The peak for Siha cells was seen after 12 hours (33%±0.6, p=0.001) while it for Hela came after just 8 hours (60%±2, p=0.028) with almost twice the amplitude. A second peak is also seen for the Hela cells. This indicated that cells move through the cell cycle to some extent after radiation with 8 Gy, but the majority have been too damaged to continue repeated cell cycles. The survival fractions for Hela cells at 8 Gy also show that most of the cells did not form colonies after receiving a radiation dose of 8 Gy.

The G2 arrest is at a maximum in Hela cells at earlier times (12-24 hours) that in Siha cells (30 hours). This is consistent with the findings in the growth curve experiment, where the Siha cells were found to have a longer doubling time than Hela. The G2 arrest is also discovered to be briefer in Hela cells than in Siha; another finding that emphasizes that Hela cells are more radiosensitive that Siha.

3.2.4 CKS2 protein content different times after irradiation with 8 Gy

Figure 30 shows that all phases seemed to have an increased level of CKS2 protein 6-8 hours after radiation in Hela cells, before returning to the levels detected in non-irradiated cells. 30 hours after radiation there seemed to be a second increase in CKS2 protein content in M phase, together with a decrease in G1 and S phase.

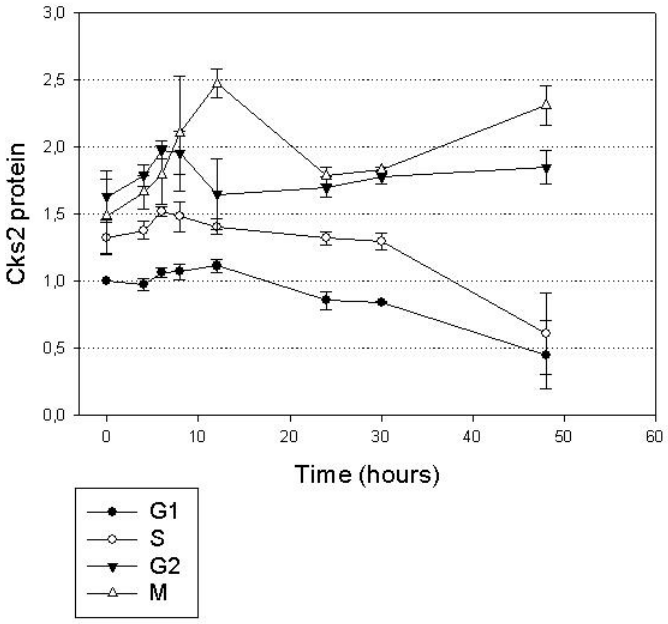

Figure 30. *CKS2 protein content in Hela cells as a function of time after radiation with 8 Gy. The measured CKS2 protein content is shown for the different phases of the cell cycle separately. The cells were fixed in methanol. Each point is the mean of three separate experiments. The bars represent standard error.*

There were no detected increases in CKS2 protein content in G1, S or G2 phase. A decrease was detected in CKS2 protein content in G1, 30 hours after radiation with 8 Gy ($p=0.002$), but with no further change after 48 hours.

In M phase, there was an increase in CKS2 protein content 12 hours after radiation ($p=0.029$). After 24 hours a subsequent decrease is detected ($p=0.005$), to a level that did not differ from the one observed in the control cells ($p=0.351$). 30 hours after radiation, there is no change from the levels detected after 24 hours ($p=0.526$), but from 30 to 48 hours after radiation there is once again an increase in CKS2 protein content in the cells ($p=0.030$). The CKS2 protein content levels detected 12 hours after-, and 48 hours after radiation was the same ($p=0.424$).

Figure 31 shows the same initial pattern in CKS2 protein expression in Siha cells as that observed for the Hela cells. There seems to be an increase in CKS2 protein levels after 8 hours for G1, S and G2 phase. No cells were detected in M phase until 24 hours after radiation. At 24 hours, the levels of CKS2 protein in M phase seemed to be increased.

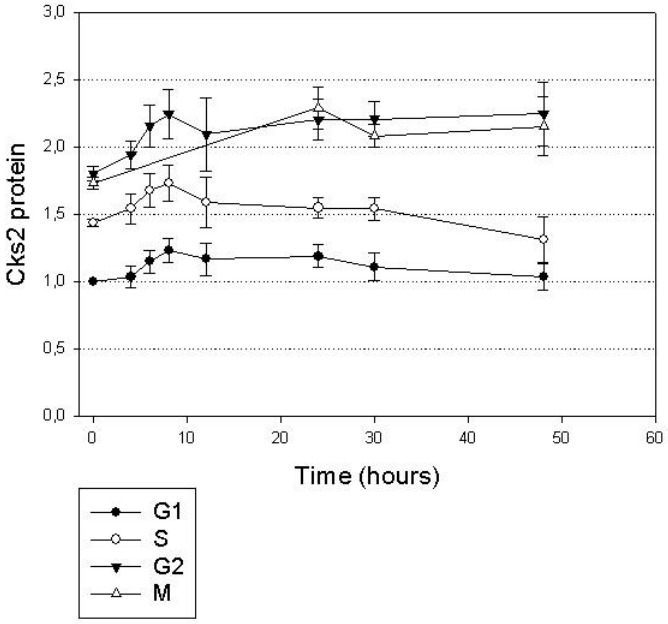

Figure 31. *CKS2 protein content in Siha cells as a function of time after radiation with 8 Gy. The measured CKS2 protein content is shown for the different phases of the cell cycle separately. The cells were fixed in methanol. Each point is the mean of three separate experiments. The bars represent standard error.*

There was no significant change in CKS2 protein content in G1 or S phase at any time after radiation. An increase in CKS2 protein in the cells in G2 phase was observed 30 hours after radiation ($p=0.046$). There was no change at 48 hours. The levels of CKS2 protein detected in the cells in M phase 24 hours after radiation were significantly higher compared to the control cells ($p=0.026$). No subsequent decrease in CKS2 protein levels were detected in the cells in M phase.

There were no changes in CKS2 protein content in cells in S phase in any of the cell lines. A decrease was detected in G1 phase 30 hours after radiation for the Hela cells. The CKS2 protein content in G1 phase in Siha cells was unaffected. In G2 phase in Siha cells, an increase was detected 30 hours after radiation. The G2 phase for Hela cells was unaffected. There were fluctuations in the CKS2 protein content in cells in M phase at different times for the two cell lines.

3.2.5 Localization of the CKS2 protein

Photos of methanol fixed Siha cells stained with anti-CKS2 and FITC conjugated secondary antibody are shown in fig 32.

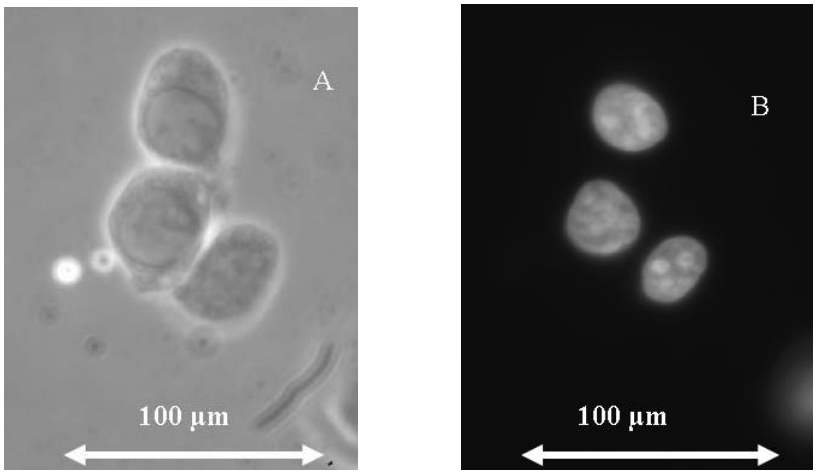

Figure 32. *Methanol fixed Siha cells in G1 phase showing the nucleus in each cell (A) and the emitted FITC fluorescence observed from the same objective (B). The objective was not moved between the two photos. Light microscopy was used.*

The observed FITC fluorescence/CKS2 protein seemed to be restricted to the nucleus. The fluorescence was observed as small dots, not evenly distributed in the nucleus. This suggests that the CKS2 protein is bound to another cellular component that is localized in specific regions of the cell/nucleus.

3.2.6 CKS2 protein content in LFM fixed cells

Figure 33 shows the CKS2 protein content measured in non-irradiated cells after LFM fixation.

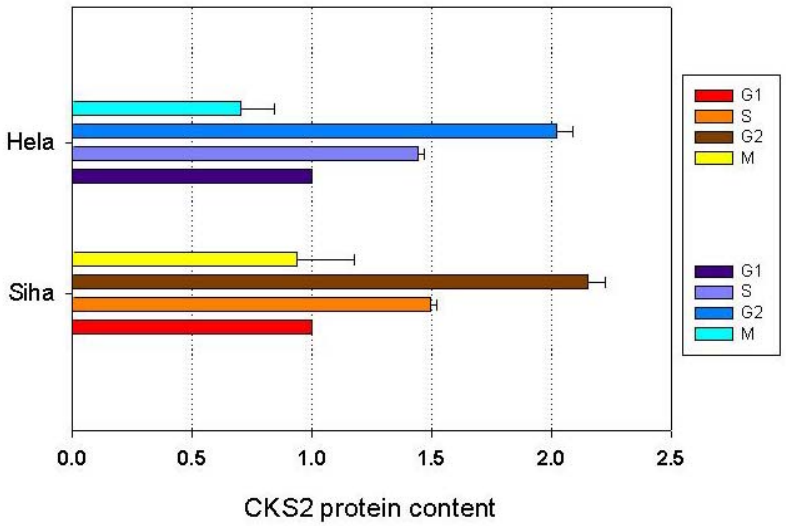

Figure33. *Bar chart showing the detected variation in CKS2 protein content in non-radiated cells in the different phases of the cell cycle in the two cell lines after LFM fixation. The results of three separate experiments are shown for each cell line. The bars represent standard errors.*

The levels of CKS2 protein in Hela cells is significantly different in S and G2 phase, compared to that in G1 phase (p=0.003 and p=0.005 respectively) and to each other. However, the levels detected in M phase after LFM fixation is comparable to that in G1 phase (p=0.170).

The same applied to Siha cells. Comparing the amount of CKS2 protein measured in G1 to that in S and G2 phase, the levels are higher in both phases (p=0.004 for both). M phase and G1 phase do not seem to differ on the basis of CKS2 protein content in LFM fixed cells.

A distribution of CKS2 protein content in the different phases of the cell cycle in non-irradiated control cells is different in LFM fixed cells than that detected in methanol fixed cells (section 3.2.6).

DISCUSSION

4.1 Experimental considerations

4.1.1 The model system

The cervical carcinoma cell lines were cultured in a controlled microenvironment where the experimental conditions were optimal and equal to all cells. Because of this, the cultured cells can be expected to have the same response to radiation. The microenvironment in human tumors is impaired, and an uneven access to nutrients and oxygen is common. This can cause heterogeneous effects of radiation in the different parts of the tumor. In immortalized cell lines that have grown in culture over a long period of time, there is also a small risk that they have changed characteristics to such an extent that they are no longer representative for the tissue from which they first originated.

For these reasons, results obtained from the model systems are not immediately comparable to the actual responses in human cancers. The results can however be indicative and motivate for further research. Promising results found in such model systems help to formulate a hypothesis. The hypothesis needs to be tested on several levels of research before it is tested on humans.

4.1.2 Overlap in FITC emission spectrum and PE excitation spectrum

There is an overlap of the FITC emission spectrum and the PE excitation spectrum (figure 34). One could therefore assume that the emission from the FITC signal would lead to further excitation of PE. This would result in a reduction in the detected signal from FITC and an increase for PE. There would be a transfer of energy from FITC to PE. Applied to experiments in this thesis, this would lead to an underestimation of CKS2 protein content. The underestimation would in theory be increasing with increasing CKS2 protein content. There would also theoretically be an increase in the detected fraction of

cells in mitosis due to a higher PE signal. Still, this is not the main concern since cells in M phase were not quantified in these experiments.

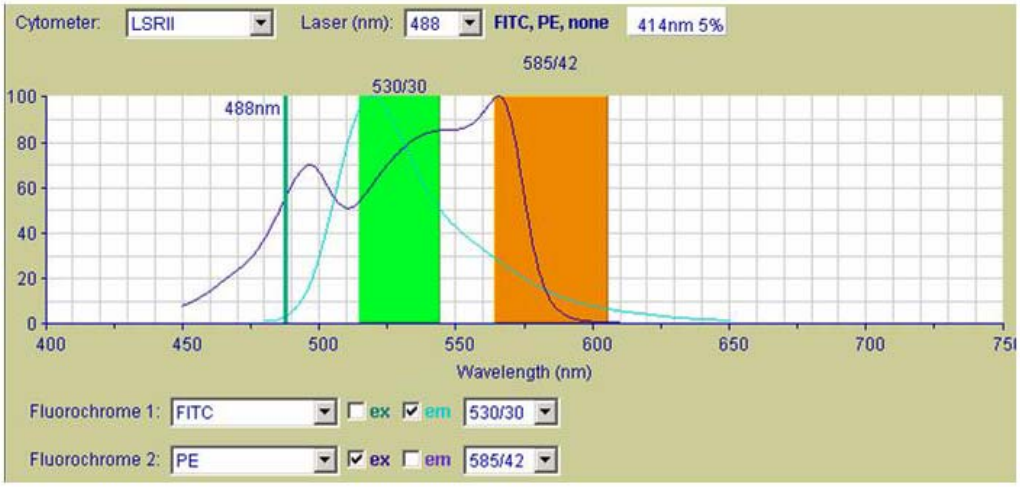

Figure34. *Spectra showing the emission of FITC (light blue line) and the excitation of PE (dark blue line). The wavelengths of the filters associated with the detectors set to record the two signals are also shown (orange and green areas), together with the laser used to excite the two fluorochromes.*

To examine if these to fluorochromes affected each other in this way, an additional control was prepared together with the original samples in one experiment of methanol fixed cells. This control was not dyed with a secondary antibody with conjugated PE, but was otherwise prepared as the “main sample” described in table A2 in appendix 11. If the presence of PE had reduced the FITC signal, the detection of FITC signal in this control sample should have been higher than the sample containing all primary and secondary antibodies. This was not the case. The overlap of spectra had therefore no effect on the detected CKS2 protein content.

One of the parameters affecting the event of such a transfer of energy between two fluorochromes is the distance between the fluorochromes in the cells. If the two fluorochromes were bound to cellular components localized very close to each other, the energy transfer had more likely occurred. The results of this control in the experiment then also give an indication on the CKS2 protein localization in the cell. In M phase, it can not be localized close to the histon complex.

4.1.3 Modfit analysis

The DNA histograms were processed with the Modfit software program to quantify the fraction of cells in the phases G1, S and G2-M. Since this analysis has been manual and done separately for each histogram, there may have been variations in the adjustments made for fitting the phases to the histograms. All analyses were performed by the same person, so these variations can be considered to be minor.

There were difficulties when analyzing the cell cycle distribution of Hela cells 48 hours after radiation with 8 Gy. In these there is, in addition to peaks for G1 and G2 phase, a third peak representing cells in S phase. The Modfit program is not designed for analyzing histograms with this abnormal distribution of cells in S phase. However, an analysis was made also for these. A manual calculation was also done on the basis of the histograms. The results from the Modfit analysis to a great extent coincided with the manually calculated fractions of cells from the histograms. Still, these numbers are presented with a higher level of uncertainty than those for the histograms just analyzed in Modfit without need for further verification.

4.1.4 Normalization of CKS2 protein content

The CKS2 protein content was normalized against the content of G1 phase in control cells. In methanol fixed cells, the CKS2 protein content is measured to be approximately ¾ higher in G2 and M phase and ½ as high in S phase compared to G1 phase in control cells. Minor variations in the cell cycle distribution of control cells between different experiments could therefore potentially cause considerable deviations if the total signal for the non-irradiated cells had been used for normalization. Additionally, the fraction of G1 is large in non-irradiated cells, and small deviations in cell fraction will therefore have little influence on the G1 signal representing CKS2 protein content. Choosing G1 phase for normalization will to the greatest extent prevent deviations from the observed values due to experimental uncertainties.

4.2 Cell line characteristics

4.2.1 The growth curve

There are variations in the doubling times for the two cell lines in previously publicized studies [40;41]. The results found in this work is in agreement with some articles [40], but not with others [41]. Cell culturing can be done under different experimental conditions, and growth rates can therefore not be expected to always coincide. However, the results from the experiments in this thesis showed a longer doubling time for Siha than for Hela. This is in agreement with other sources [40].

There is a discrepancy between the cell density reached for the Hela cells in this work (<40,000 cells/cm^2) and the cell densities stated for splitting (70-80.000 cells/cm^2). When Hela cells were cultured, medium was just shifted or added to the culturing flask if the cells had not reached confluency. When replacing or adding medium in this way, the Hela cells managed to grow in much more crowded environments than the maximum level observed in the experiment concerning the growth curve. In the growth curve experiment, no medium was added or shifted. Had this been done, the Hela cells would probably have reached much higher cell densities (>80,000 cells/cm^2) in this work.

4.2.2 Clonogenic assay and radiosensitivity

The calculated PE for Hela and Siha cells was not significantly different. The PE found for Hela cells was in agreement with other sources [40]. Work described in previous publications had found a higher PE for Siha cells than what was found in the experiment in this thesis [40]. These other findings had been made under slightly different experimental conditions. The medium was different, as was the number of cells initially seeded and the incubation time. All these factors may have influenced the ability to form colonies and hence the PE.

It was found that Hela cells were more radiosensitive than Siha. This is in agreement with previous publications [40;42]. The survival fractions calculated were also to a large

extent in accordance to that described in other sources [40;42;43]. These sources also confirmed that the difference in radiosensitivity in the two cell lines is increasing with increasing radiation doses.

4.3 Effects of radiation on cell cycle distribution

4.3.1 Changes in cell cycle distribution 24 hours after different radiation doses

These experiments were preformed to identify a G2 arrest after radiation and at which dose it was first detected. The response to radiation was found to be similar in the two cell lines. There was a decrease in the fraction of cells in G1 phase with increasing radiation doses. There was a corresponding increase in the fraction of cells in G2-M phase, while the fraction of cells in S phase was unaffected by radiation. The changes in cell fractions in G1 and G2-M were first seen after 4 Gy.

The increase of cells in G2-M phase was the result of cells arresting in G2 due to activation of the G2 checkpoint by the radiation induced DNA damage. The arrest is thought to give time to repair the damage before cell division or mediate cell death [11;28]. More cells are damaged with increasing doses of ionizing radiation, explaining the higher fraction of cells arrested in G2 at higher radiation doses. The findings concerning cell cycle distribution in response to radiation with different doses is in agreement with previously publicized results [41;44].

4.3.2. Changes in cell cycle distribution different times after irradiation with 8 Gy

There were similarities between the two cell lines concerning cell cycle distribution after different times after irradiation with 8 Gy. A large fraction of cells from G1 and S phase moved through cycle and arrested in G2 after radiation. The graphs showing fraction of cells in G1 had no plateau before a minimum was reached. This indicates that there was little or no G1 arrest in response to ionizing radiation in either of the two cell lines. HPV

infected cervical carcinoma cells lose their G1 checkpoint, probably due to degradation of TP53 and RB1 by the viral oncoproteins E6 and E7, respectively. The found results were therefore in agreement with previous publications [21;23;24;41].

The fraction of cells in S phase was observed to increase 4-12 hours after radiation for both cell lines. This is a retardation of cells through S phase in response to damages inflicted by ionizing radiation. This observation was also in accordance with previous work on cervical carcinoma cell lines [41].

The number of cells in G2-M increased after radiation for both cell lines. A maximum level was reached after 24-30 hours. These were cells arresting in G2 phase after radiation induced activation of the checkpoint. The cell fraction of Hela cells in G2 phase subsequently decreased after 30-48 hours, indicating an abolishment of the arrest. For Siha cells, the fraction of cells representing the maximum G2 arrest at 30 hours was not significantly decreased after 48 hours. Still, since the fraction of cells in G1 phase increased, the G2 arrest could also be considered abolished in the Siha cells 48 hours after irradiation.

There could be speculations that these observations were the result of selective cell death from G2 or M phase. However, M phase Siha cells are first detected 24 hours after radiation, while Hela cells in M phase can be detected at all times after irradiation. This indicated that the cells passed through the G2 checkpoint. Also, in the radiosensitivity experiment, there were many colonies with numbers of cells below the set threshold. This indicated that the cells start proliferating after a G2 arrest, but lose their reproductive ability after a few cycles. Additionally, dead cells would be detected as debris in the flow cytometry analysis. The detected debris was slightly higher after 48 hours, but was still considered to be negligible. The increased cell fraction in G1 phase and the reduced cell fraction in G2 can therefore be said to be the result of an abolished G2 arrest and not due to selective cell death form G2 or M phase. This was in agreement with other references [21;24;41].

It is suggested that TP53 has a role in maintenance of the arrest in the G2 checkpoint and that the observed abolishment of the arrest observed in HPV positive cells are due to E6 mediated degradation of TP53 [21;24;29]. However, cells with defects in the TP53 pathway are seen to arrest permanently in G2 after irradiation [38]. The causes for the observed abolished G2 arrest are therefore unclear.

For all phases in both the cells lines, the fraction of cells in the different phases at 48 hours after radiation showed a tendency of returning, or had returned, to the levels detected in control cells. In Hela cells, however, there was a second accumulation of cells in S phase with the shape of a peak close to the cells in G2-M phase. The observed uneven distribution of cell in S phase was different from the retardation observed 4-24 hours after irradiation.

This peak in S phase could possibly consist of synchronized cells from G2 phase at the time of radiation, which started proliferating simultaneously after the arrest. It is only observed for the Hela cells after 48 hours. The same result may have been obtained for the Siha cells had they been harvested and fixed at a later time. Since the Hela cells were found to move faster through cycle than the Siha cells in the growth curve experiment, this can be considered a reasonable assumption. In the radiosensitivity experiment, low survival fraction after 8 Gy is observed for both cell lines. The majority of cells analyzed with flow cytometry at different times after exposure to this radiation dose were therefore dying. The cell cycle distribution 48 hours after irradiation probably illustrates the progressing difficulties the cells have moving through cell cycle after irradiation.

4.4 Effects of radiation on CKS2 protein content

4.4.1 CKS2 protein content 24 hours after different radiation doses

An increase in CKS2 protein was seen in M phase for both cell lines with increasing radiation doses. For Hela cells there was also shown an increase in CKS2 protein content in G2 phase cells. The graphs showed a similar trend for Siha cells, but it was not

significant. If more parallels had been performed, this may have been clarified. There are no previously published results to compare these findings to. It is not yet known if the role of CKS2 in the cell cycle is somehow linked to the changes of phenotype seen in the cervical carcinoma cells after radiation. It is, nevertheless possible to speculate on what these findings could indicate. For the further discussion, it is assumed that there was an increase in CKS2 protein content in both G2 and M phase with a corresponding G2 arrest with increasing radiation doses.

It is suggested that CKS2 is important for the G2-M transition [14;15]. In relation to this, a hypothesis can be made that the increase in CKS2 protein with increasing radiation dose is a cellular signal due to (a) positive feedback mechanism(s). This feedback is activated as a cellular response in cells arrested in G2 phase after radiation. The signal is given so that the arrested cells can move through the G2 checkpoint and continue proliferation.

Considering the survival fraction of both cell lines at high radiation doses, most cells analyzed with flow cytometry after radiation have serious DNA damage. Experiments in this thesis showed that the G2 arrest after radiation was eventually abolished. An assumption can be made that the DNA damage inflicted on the cells by radiation had not been completely repaired when the G2 arrest was abolished. In that sense, the increased levels of CKS2 protein can be seen as a lack of negative feedback mechanism(s). If the CKS2 protein content had not increased, the cells may have been arrested in G2 until DNA damage had been repaired.

Further research is needed to determine the role of CKS2 as a regulator of cell cycle and its functions in radiation response. This may just as easily disprove these hypotheses as confirm them.

4.4.2 CKS2 protein content different times after irradiation with 8 Gy

Changes in CKS2 protein content was detected for both cell lines. For all phases, the graphs showed an increase 6-12 hours after radiation. The increase was significant only in M phase in Hela cells. Siha cells in M phase were first detected 24 hours after irradiation, and they had significantly increased CKS2 protein levels. If more parallels had been performed, significant initial increases in CKS2 protein levels may have been shown for other phases too. The observed increase was returned to approximately normal levels in Hela cells before the maximum fractions of cells in G2 phase were observed. The levels of CKS2 protein observed in Siha cells in M phase were unchanged between 24-48 hours after irradiation. An increase was also seen after 30 hours in G2 phase for the Siha cells. There seems to be no connection between these results and the observed decrease in CKS2 protein levels in G1 phase for Hela cells. This finding was therefore overruled.

If the response to radiation leads an immediate increase in expression of the gene coding for the CKS2 protein, it will take some time before the protein is translated. There will also be a delay between detection of the protein in the cell and the results of its functions. So even if a time period was observed between the maximum CKS2 protein content and G2 arrest, the hypothesis stated in the previous section can still be used to explain these results. Further research is needed before any of these explanations can be considered valid.

4.5 *CKS2 protein conformation and localization*

When cells are LFM fixed, they are lysed. All staining of the CKS2 protein and flow cytometry analysis was therefore done on nucleoli. Since these results were not different for G1, S and G2 phase from those detected in methanol fixed cells, the CKS2 protein must be localized in the nucleus as long as the nuclear membrane is intact. The results from the light microscopy also suggested that the CKS2 protein was localized in the nucleus. This is in agreement with results found in plant cells with a CKS2 protein analogue [16].

Lysing cells in M phase would in theory suspend the nuclear content in the detergent buffer since there is no intact membrane to enclose them. However, the chromosomes and other nuclear components remain attached to one another and can be detected as distinct units[39]. The mechanism for this is unclear.

The detected CKS2 protein content in M phase after LFM fixation was similar to levels detected in G1 phase (section 3.2.2). In he samples that were methanol fixed, the CKS2 content of the cells in M phase was equal to that detected in G2 phase (section 3.2.6). The detected CKS2 protein content in M phase is much lower after LFM fixation compared to methanol fixation. Slight variations are also seen in the G2 phase of the cell cycle when comparing methanol- and LFM fixed cells, but not nearly to the same extent. The CKS2 protein content measured in G1 and S phase after the two fixation methods are equal. This could possibly indicate a change in conformation of the CKS2 protein in M phase.

Suspending cells in detergent buffer and subsequently adding formaldehyde has been shown to extract hyperphosphorylated pRB1 from cells in S, G2 and M phase, but not from G1 phase [45]. This is due to pRB1's change in conformation. Applying these findings to the results from the presented work, it is possible to assume that the CKS2 protein has a different conformation in M phase compared to interphase and that this is the reason for the decreased M phase signal after LFM fixation.

4.6 Further research

Several of the goals described in the introduction have been reached in the experiments in this thesis. One of the goals where the results remained inconclusive, were the linking of CKS2 protein fluctuations to cell cycle distribution after radiation. Further research to elucidate the role of CKS2 in radiation response must be performed. Observing changes in cell cycle distribution after radiation in cells where CKS2 protein expression is intervened, could further suggest the role of CKS2 in radiation response. Intervention

could be over- or underexpression of the gene or protein. The specific localization of the CKS2 protein also needs to be further investigated in addition to its conformational changes throughout the cell cycle.

4.7 Conclusions

The two cell lines were established in the department laboratory and the results described in this thesis give information on growth rate, PE and radiosensitivity. This can be useful for designing future radiobiological studies. The changes in cell cycle distribution in response to radiation after different doses and -times were determined for both cell lines. A suitable method was developed for detecting CKS2 protein content in all phases of the cell cycle separately.

The levels of CKS2 protein were affected in response to radiation. The phases M and G2 are observed as the two phases of the cell cycle where the fluctuations are greatest. There are also observed changes in CKS2 protein content in G1 and S phase, but no statistically significant differences were detected. More parallels of the experiments could have revealed fluctuations in CKS2 protein content also in these phases.

Attempts to link the changes in CKS2 protein content to cell cycle distribution after radiation, was attempted in the discussion. The results remain inconclusive. Further research is needed to clarify the role of the CKS2 protein in response to radiation as well as its role as a regulator of the cell cycle.

The localization of the CKS2 protein was observed to be restricted to the nucleus. Conformational changes of the CKS2 protein in interphase and M phase is indicated. Further research is needed to determine the localization of CKS2 in the cell and it’s interaction with other cellular components in the different parts of the cell cycle.

REFERENCE LIST

[1] Alberts, Johnson, Lewis, Raff, Roberts, Walter: Cancer; in Gibbs S (ed): Molecular Biology Of The Cell. New York, Garland Science, 2002, pp 1313-1347.

[2] Cannistra SA, Niloff JM: Cancer of the uterine cervix. N Engl J Med 18-4-1996;334:1030-1038.

[3] Lazo PA: The molecular genetics of cervical carcinoma. Br J Cancer 1999;80:2008-2018.

[4] Wong YF, Cheung TH, Tsao GS, Lo KW, Yim SF, Wang VW, Heung MM, Chan SC, Chan LK, Ho TW, Wong KW, Li C, Guo Y, Chung TK, Smith DI: Genome-wide gene expression profiling of cervical cancer in Hong Kong women by oligonucleotide microarray. Int J Cancer 15-5-2006;118:2461-2469.

[5] Hougardy BM, van der Zee AG, van den Heuvel FA, Timmer T, de Vries EG, de JS: Sensitivity to Fas-mediated apoptosis in high-risk HPV-positive human cervical cancer cells: relationship with Fas, caspase-8, and Bid. Gynecol Oncol 2005;97:353-364.

[6] Milde-Langosch K, Riethdorf S: Role of cell-cycle regulatory proteins in gynecological cancer. J Cell Physiol 10-8-2003;196:224-244.

[7] Tommasino M, Accardi R, Caldeira S, Dong W, Malanchi I, Smet A, Zehbe I: The role of TP53 in Cervical carcinogenesis. Hum Mutat 2003;21:307-312.

[8] Treatment of cervical cancer in Norway. Det Norske Radiumhospital . 10-5-2006.
Ref Type: Internet Communication

[9] Lyng H, Brovig RS, Svendsrud DH, Holm R, Kaalhus O, Knutstad K, Oksefjell H, Sundfor K, Kristensen GB, Stokke T: Gene expressions and copy numbers associated with metastatic phenotypes of uterine cervical cancer. BMC Genomics 2006;%20;7:268.

[10] Alberts, Johnson, Lewis, Raff, Roberts, Walter: The Cell Cycle And Programmed Cell Death; in Gibbs S (ed): Molecular Biology Of The Cell. New York, Garland Science, 2002, pp 983-1010.

[11] Kastan MB, Bartek J: Cell-cycle checkpoints and cancer. Nature 18-11-2004;432:316-323.

[12] Sherr CJ: The Pezcoller lecture: cancer cell cycles revisited. Cancer Res 15-7-2000;60:3689-3695.

[13] Vermeulen K, Van Bockstaele DR, Berneman ZN: The cell cycle: a review of regulation, deregulation and therapeutic targets in cancer. Cell Prolif 2003;36:131-149.

[14] Egan EA, Solomon MJ: Cyclin-stimulated binding of Cks proteins to cyclin-dependent kinases. Mol Cell Biol 1998;18:3659-3667.

[15] Pines J: Cell cycle: reaching for a role for the Cks proteins. Curr Biol 1-11-1996;6:1399-1402.

[16] Hepler PK, Sek FJ, John PC: Nuclear concentration and mitotic dispersion of the essential cell cycle protein, p13suc1, examined in living cells. Proc Natl Acad Sci U S A 15-3-1994;91:2176-2180.

[17] Urbanowicz-Kachnowicz I, Baghdassarian N, Nakache C, Gracia D, Mekki Y, Bryon PA, Ffrench M: ckshs expression is linked to cell proliferation in normal and malignant human lymphoid cells. Int J Cancer 2-7-1999;82:98-104.

[18] Spruck CH, de Miguel MP, Smith AP, Ryan A, Stein P, Schultz RM, Lincoln AJ, Donovan PJ, Reed SI: Requirement of Cks2 for the first metaphase/anaphase transition of mammalian meiosis. Science 25-4-2003;300:647-650.

[19] Figure showing a schematic overview of the female reproductive organ. Health care at West Virginia University . 10-5-2006.
Ref Type: Internet Communication

[20] Cell types in the cervix and development of cancer. Womens Health Alliance . 10-5-2006.
Ref Type: Internet Communication

[21] Thomas M, Pim D, Banks L: The role of the E6-p53 interaction in the molecular pathogenesis of HPV. Oncogene 13-12-1999;18:7690-7700.

[22] Norwegian prevalence of precursor lesions and cervical cancer. Kreftforeningen . 10-5-2006.
Ref Type: Internet Communication

[23] DeWeese TL, Walsh JC, Dillehay LE, Kessis TD, Hedrick L, Cho KR, Nelson WG: Human papillomavirus E6 and E7 oncoproteins alter cell cycle progression but not radiosensitivity of carcinoma cells treated with low-dose-rate radiation. Int J Radiat Oncol Biol Phys 1-1-1997;37:145-154.

[24] Thompson DA, Belinsky G, Chang TH, Jones DL, Schlegel R, Munger K: The human papillomavirus-16 E6 oncoprotein decreases the vigilance of mitotic checkpoints. Oncogene 18-12-1997;15:3025-3035.

[25] Cho NH, Kim YT, Kim JW: Alteration of cell cycle in cervical tumor associated with human papillomavirus: cyclin-dependent kinase inhibitors. Yonsei Med J 2002;43:722-728.

[26] Eric J Hall: The Physics And Chemistry Of Radiation Absorption; in Radiobiology For The Radiobiologist: Philadelphia, Lippincott Williams & Wilkins, 2006, pp 5-16.

[27] Ricci MS, Zong WX: Chemotherapeutic approaches for targeting cell death pathways. Oncologist 2006;11:342-357.

[28] Ishikawa K, Ishii H, Saito T: DNA damage-dependent cell cycle checkpoints and genomic stability. DNA Cell Biol 2006;25:406-411.

[29] Roninson IB, Broude EV, Chang BD: If not apoptosis, then what? Treatment-induced senescence and mitotic catastrophe in tumor cells. Drug Resist Updat 2001;4:303-313.

[30] Intoduction To Flow Cytometry: A Learning Guide. BD Bioscience . 2006.
Ref Type: Internet Communication

[31] BD LSR II User's Guide. BD Bioscience . 2006.
Ref Type: Internet Communication

[32] Fluorescence Spectrum Viewer. BD Bioscience . 2006.
Ref Type: Internet Communication

[33] Alberts, Johnson, Lewis, Raff, Roberts, Walter: Manipulating Proteins, DNA, And RNA; in Gibbs S (ed): Molecular Biology Of The Cell. New York, GArland Science, 2002, pp 476-478.

[34] Hela Cell Line. LGC Promochem . 2006.
Ref Type: Internet Communication

[35] Siha Cell Line. LGC Promochem . 2006.
Ref Type: Internet Communication

[36] Begg A.C., Gordon Steel G.: Cell proliferation and growth rate of tumours; in Gordon Steel G. (ed): Basic Clinical Radiobiology. New York, Edward Arnold (Publishers) Ltd., 2002, pp 8-22.

[37] Eric J Hall: Cell Survival Curves; in John J-R., Sutton P., Marino D. (eds): RADIOBIOLOGY FOR THE RADIOBIOLOGIST. Philadelphia, Lippincott Willians & Wilkins, 2000, pp 32-50.

[38] Landsverk KS, Lyng H, Stokke T: The response of malignant B lymphocytes to ionizing radiation: cell cycle arrest, apoptosis and protection against the cytotoxic effects of the mitotic inhibitor nocodazole. Radiat Res 2004;162:405-415.

[39] Larsen K.L., Munch-Pettersen B., Christiansen J., Jørgensen K.: Flow Cytometric Discrimination of Mitotic Cells: Resolution of M, as Well as G1, S and G2 Phase With Mithramycin, Propidium Iodide, and Ethidium Bromide After Fixation With Formaldehyde. CYTOMETRY 18-7-2006;7:54-63.

[40] Banath JP, Macphail SH, Olive PL: Radiation sensitivity, H2AX phosphorylation, and kinetics of repair of DNA strand breaks in irradiated cervical cancer cell lines. Cancer Res 1-10-2004;64:7144-7149.

[41] Ree AH, Stokke T, Bratland A, Patzke S, Nome RV, Folkvord S, Meza-Zepeda LA, Flatmark K, Fodstad O, Andersson Y: DNA damage responses in cell cycle G2 phase and mitosis--tracking and targeting. Anticancer Res 2006;26:1909-1916.

[42] Sheridan MT, West CM: Ability to undergo apoptosis does not correlate with the intrinsic radiosensitivity (SF2) of human cervix tumor cell lines. Int J Radiat Oncol Biol Phys 1-6-2001;50:503-509.

[43] Tam KF, Ng TY, Liu SS, Tsang PC, Kwong PW, Ngan HY: Potential application of the ATP cell viability assay in the measurement of intrinsic radiosensitivity in cervical cancer. Gynecol Oncol 2005;96:765-770.

[44] Mose S, Class R, Weber HW, Rahn A, Brady LW, Bottcher HD: Radiation enhancement by gemcitabine-mediated cell cycle modulations. Am J Clin Oncol 2003;26:60-69.

[45] Stokke T, Erikstein B.K, Smedshammer L., Boye E., Steen H.: The Retinoblastoma Gebe Product Is Bound in the Nucleus in Early G1 phase. Experimental Cell Research 1993;204:147-155.

APPENDIX

APPENDIX 1: Protocol for thawing cells

APPENDIX 2: Protocol for splitting cells

APPENDIX 3: Protocol for freezing cells

APPENDIX 4: Protocol for the growth curve experiment

APPENDIX 5: Protocol for seeding out cells for the clonogenic assay and the Radiosensitivity experiment

APPENDIX 6: Protocol for fixating and dying colonies

APPENDIX 7: Protocol for harvesting cells

APPENDIX 8: Protocol for fixating cells

APPENDIX 9: Protocol for preparing the detergent buffer (“Larsen”)

APPENDIX 10: Protocol for the experiments showing effects on cells after radiation with different doses or different times after radiation

APPENDIX 11: Protocol for staining cells for flow cytometry analysis

APPENDIX 12: Protocol for running and analyzing samples with the LSR II

APPENDIX 13: The combinations of fluorochromes, lasers, filters and detectors used for my work

APPENDIX 14: Reagents used in the experiments

APPENDIX 1

Protocol for thawing cells

1. Heat cell culturing medium in a heat bath till the temperature is about 37°C.
2. Fetch one cryotube with cells from the freezer (-80°C for short time storage < 1 year) or from the liquid nitrogen tank (ca -200°C for long time storage > 1 year).

In a LAF bench using aseptic procedures:

3. Thaw the content of the cryotube by alternately adding and removing small volumes of preheated medium to the cryotube, about 3.5 ml, with a 5 ml pipette until there is no more ice in the cryotube.
4. Add the medium containing the thawed cells from the 5 ml pipette to a 15 ml tube.
5. Centrifuge the suspension for 5 min at 1100 rpm/min at room temperature.
6. Remove the supernatant with a pasteur pipette connected to water suction.
7. Resuspend the cell pellet in 15 ml of preheated medium and transfer to a T_{75} cell culturing flask.
8. Incubate the flask in a 37°C humified atmosphere containing 5 % CO_2 in air.
9. Split cells when necessary.

APPENDIX 2

Protocol for splitting cells

1. Heat cell culturing medium and trypsin-EDTA in a heat bath till the temperature of both solutions is about 37°C.

In a LAF bench using aseptic procedures:

2. Remove medium and wash once with a small volume of trypsin-EDTA (about 1 ml for a T_{25} flask, 2 ml for a T_{75} flask).
3. Remove trypsin-EDTA immediately after wash using a pasteur pipette connected to water suction.
4. Once again, add a small volume of trypsin-EDTA but this time wait for cell detachment. Detachment will be promoted by incubating of the cell flask(s) at 37°C for a couple of minutes, the time being dependent on cell confluency, the type of cell line and the activity of the enzyme. A firm knock or two on the side of the flask will further promote the cell detachment.
5. Add about 5 ml of preheated medium to the flask for inhibiting further activity of the trypsin-EDTA solution. Disperse the cells in the added medium by pipetting.
6. Add the cell suspension to a tube.
7. Centrifuge the suspension for 5 min at 1100 rpm/min at room temperature.
8. Remove the supernatant with a pasteur pipette connected to water suction.
9. Resuspend the cell pellet in preheated medium.
10. Distribute the cells into new flasks in a suitable ratio (about 2-3 million cells in T_{75} flasks and about 0.5-1 million cells in T_{25} flasks) depending on the original confluency. Add preheated medium to the flasks so that total volume adds up to 12-15 ml in a T_{75} flask and 5-7 ml in a T_{25} flask.
11. Incubate the flasks in a 37°C humified atmosphere containing 5 % CO_2 in air.

APPENDIX 3

Protocol for freezing cells

1. Heat FBS in a heat bath until it has been thawed, and also trypsin-EDTA and cell culturing medium until the temperature is about 37°C.

In a LAF bench using aseptic procedures:

2. Make a “cell freezing solution” containing 90% FBS and 10 % DMSO. Put this solution in the refrigerator and keep cool until it is about to be used.
3. Remove medium from the cell flask(s), wash once with trypsin-EDTA, add trypsin-EDTA for cell detachment, neutralize with preheated medium and centrifuge and remove supernatant as previously described.
4. Resuspend the cell pellet(s) in the “cell freezing solution” taken directly from the refrigerator into the LAF bench. Solution volume depends on the number of cryotubes and the cell concentration. (A suitable amount of cells to freeze in one cryotube is 4-5 million cells, but this is a highly flexible number. Furthermore, a cryotube can usually contain 1.5-2 ml of fluid.)
5. Put premarked cryotubes into a transportable freezing block that keeps a temperature of -20°C. Fill the cryotubes with the suitable volume of the cell suspension.
6. Transport the cryotubes in the freezing block as quickly as possible to the freezer or the liquid nitrogen tank depending on assumed storage time as described in the “thawing cells” procedure.

APPENDIX 4

Protocol for the growth curve experiment

1. Perform the steps 1-8 in the protocol for splitting cells in appendix 2 with a culturing flask containing sufficient numbers of cells in (assumed) exponential growth.
2. Resuspend the cell pellet in 30 ml preheated medium.
3. Measure the number of cells pr. ml. cell suspension by using the colter counter. Use the mean of three separate outtakes.
4. Calculate the volume of cell suspension that gives 50,000 cells for Hela and 75,000 cells for Siha.
5. Seed out the calculated volume into 54 separate T_{25} flasks.
6. Add preheated medium to give the final volume of 5 ml in each cultivating flask.
7. Incubate the flasks in a 37°C humified atmosphere containing 5 % CO_2 in air.
8. Perform the steps 1-8 in the protocol for splitting cells in appendix 2 with three of the T_{25} flasks each following day.
9. Resuspend the cell pellet in a suitable volume.
10. Take three separate outtakes of each tube.
11. Count the number of cells pr ml in a colter counter. The mean of the three separate outtakes is representative for the cell number in one of the flasks. These values give rise to the points and error bars plotted in the graph.
12. Repeat steps 8-11 until confluent phase is definitely reached.

APPENDIX 5

Protocol for seeding out cells for the clonogenic assay and the radiosensitivity experiment

1. Perform the steps 1-8 in the protocol for splitting cells in appendix 2 with a culturing flask containing sufficient numbers of cells in exponential growth.
2. Resuspend the pellet in 20 ml medium.
3. Measure the number of cells pr. ml. cell suspension by using the colter counter. Use the mean of three separate outtakes.
4. Calculate the volume of suspension that corresponds to predetermined cell numbers. Dilute the initial cell suspensions so that the volume seeded into each flask is larger than 0.3 ml for sufficiently accurate cell numbers.
5. Seed out the calculated volume into T_{25} flasks giving three parallels for each cell number.
6. Add preheated medium to give the final volume of 5 ml in each cultivating flask.
7. Incubate the flasks in a 37°C humified atmosphere containing 5 % CO_2 in air.

APPENDIX 6

Protocol for fixating and dying colonies

All solutions should be added in estimated volumes observed large enough to cover the cultivating area of each flask.

1. Pour off medium from the culturing flasks
2. Wash the colonies once in 0.9 % NaCl
3. Add 70 % ethanol which will fix the colonies instantly
4. Add a solution of Comasie Blue in 10 % acetic acid and 45 % methanol and leave for 30 minutes.
5. Remove the excess dye and rinse of the excess with tap water
6. Air dry

APPENDIX 7

Protocol for harvesting cells

This protocol is used for experiments where cells are seeded in flasks with culturing area of 25 cm^2.

1. Collect the medium from the two culturing flasks that had received the same treatment in the same 15 ml tube.
2. Add 1 ml of trypsin-EDTA to briefly wash the cells.
3. Collect the trypsin-EDTA used for washing in the same tube as the medium.
4. Add 1 ml trypsin-EDTA for cell detachment.
5. Transfer the cell suspension to the tube containing medium and the trypsin-EDTA used for washing after complete cell detachment.
6. Centrifuge the tube at 1100 rpm/min for 5 minutes at room temperature
7. Remove the supernatant with a Pasteur pipette connected to water suction
8. Fix cells in one of the two ways described in appendix 8 and store at -20ºC.

APPENDIX 8

Protocol for fixating cells

Methanol fix	LFM fix
1. Add 1-2 ml of 100 % methanol (-20ºC) to the cell pellet. 2. Make sure that all cells are suspended in the methanol by gently pipetting up and down with a pasteur- or automatic pipette. 3. Immediately transport the sample to the freezer (-20ºC)	1. Put the tube containing the cell pellet on ice. 2. Add 3 ml of detergent buffer (described in appendix 9) 3. Make sure that all cells are suspended in the fluid by gently pipetting up and down with a pasteur- or automatic pipette. Leave on ice for 5 minutes. 4. Add 1 ml of 4 % formaldehyde solution, giving a final concentration of 1 %. Leave on ice for 1 hour [38;39;45]. 5. Centrifuge at 1100 rpm/min for 5 minutes at room temperature 6. Remove the supernatant with a pasteur pipette connected to water suction. 7. Follow the procedure for methanol fixating cells.

APPENDIX 9

Protocol for preparing the detergent buffer (“Larsen”)

0.1% Igepal CA-630 (=Nonidet P40)

6.5 mM Na2PO4

1.5 mM KH2PO4

2.7 mM KCl

137 mM NaCl

0.5 mM EDTA

The buffer should have pH 7.2.

APPENDIX 10

Protocol for the experiments showing effects on cells after radiation with different doses or different times after radiation

1. Perform the steps 1-8 in the protocol for splitting cells in appendix 1 with culturing flasks containing sufficient numbers of cells in exponential growth.
2. Resuspend the pellet in 20-30 ml of preheated medium.
3. Measure the number of cells pr. ml. cell suspension by using the colter counter. Use the mean of three separate outtakes.
4. Calculate the volume of cell suspension that gives 800,000 cells for Hela and 1,200,000 cells for Siha.
5. Seed out the calculated volume into 12 or 16 T_{25} culturing flasks, depending on the experiment.
6. Add preheated medium to give the final volume of 5 ml in each cultivating flask.
7. Incubate the flasks in a 37°C humified atmosphere containing 5 % CO_2 in air.
8. Irradiate the cells with the intended dose after 24 hours.
9. Harvest and fixated the cells as described in appendix 7 at the determined times after radiation.
10. Prepare the samples for flow cytometry and analyze.

APPENDIX 11

Protocol for staining cells for flow cytometry analysis

- Perform all steps at 0ºC.
- Leave the detergent buffer with dried non-fat milk in a heat bath for one hour. Centrifuge at 3000 rpm/min for 4-5 minutes. Only use the supernatant to prepare the solutions for staining the cell samples.
- Perform all centrifugations at 1100 rpm/min at 0ºC for 10 minutes if not otherwise specified.
- The final concentrations of all reagents used in the staining procedures are listed in table A1. Prepare common solutions from which the smaller volumes are added to the sample in the following staining procedures.

Table A1. *The antibodies, fluorochromes and antibodies with conjugated fluorochromes, listed together with their final concentrations. The dilutions corresponding to these concentrations are given in parenthesis.*

Antibody/ Fluorochrome	Anti pH3	Anti Cks2	FITC	PE	Hoechst 33258	PI	RNaseA
Concentrations	2 µg/ml (1:500)	20 µg/ml (1:25)	40 µg/ml (1:25)	8 µg/ml (1:25)	1.5 µg/ml	5 µg/ml	100 µg/ml

1) Centrifuge all sample tubes and remove the methanol using a pasteur pipette connected to water suction.
2) Resuspend the cell sample in 3 ml PBS holding 2-8ºC.
3) Evenly distribute the cell suspension into 3 premarked falcon tubes.
4) Centrifuge the samples and remove the PBS using a Pasteur pipette connected to water suction.
5) One parallel from each sample is treated as described in table A2 or A3.

Table A2. *Protocol for preparing methanol fixated cells for flow cytometry*

"Main sample" Gives the value for measured CKS2 protein content	Control Measures unspecific binding of the FITC goat anti-mouse antibody	Control Measures autofluorescence Should be low enough to neglect
Mouse anti-CKS2 FITC goat anti-mouse Rabbit anti-PH3 PE goat anti-rabbit Hoechst 33258	FITC goat anti-mouse Rabbit anti-PH3 PE goat anti-rabbit Hoechst 33258	Rabbit anti-PH3 PE goat anti-rabbit Hoechst 33258
1. Resuspend pellet in 50 µl mouse anti-CKS2 and 50 µl rabbit anti-phospho histon H3, both in detergent buffer with added 4 % dried non-fat milk. 2. Leave on ice for 30 minutes. 3. Add PBS and centrifuge. 4. Resuspend the cell pellet in 50 µl FITC conjugated goat anti-mouse and 50 µl PE conjugated goat anti-rabbit, both in detergent buffer with added 4 % dried non-fat milk. 5. Leave on ice for 30 minutes. 6. Wash once in PBS 7. Add 700 µl Hoechst 33258 in PBS.	1. Resuspend pellet in 100µl rabbit anti-phospho histon H3 in detergent buffer with added 4 % dried non-fat milk. 2. Leave on ice for 30 minutes. 3. Add PBS and centrifuge. 4. Resuspend the cell pellet in 50 µl FITC conjugated goat anti-mouse and 50 µl PE conjugated goat anti-rabbit. 5. Leave on ice for 30 minutes. 6. Wash once in PBS 7. Add 700 µl Hoechst 33258 in PBS.	1. Resuspend pellet in 100 µl rabbit anti-phospho histon H3 in detergent with added 4 % dried non-fat milk. 2. Leave on ice for 30 minutes. 3. Add PBS and centrifuge. 4. Resuspend the cell pellet in 100 µl PE conjugated goat anti-rabbit in detergent buffer with added 4 % non-fat dried milk. 5. Leave on ice for 30 minutes. 6. Wash once in PBS 7. Add 700 µl Hoechst 33258 in PBS.

Table A3. *Protocol for preparing LFM fixated cells for flow cytometry*

"Main sample" Gives the value for measured CKS2 protein content	Control Measures unspecific binding of the FITC goat anti-mouse antibody	Control Measures autofluorescence Should be low enough to neglect
Mouse anti-CKS2 FITC goat anti-mouse Hoechst 33258 PI RNaseA	FITC goat anti-mouse Hoechst 33258 PI RNaseA	Hoechst 33258 PI RNaseA
1. Resuspend pellet in 100 µl mouse anti-CKS2 in detergent buffer with added 4 % dried non-fat milk. 2. Leave on ice for 30 minutes 3. Add PBS and centrifuge 4. Resuspend pellet in 100 µl FITC conjugated goat anti-mouse in detergent buffer with added 4 % dried non-fat milk. 5. Leave on ice for 30 minutes 6. Add PBS and centrifuge 7. Add 700 µl PBS containing Hoechst 33258, PI and RNaseA.	1. Resuspend pellet in 100 detergent buffer with added 4 % dried non-fat milk. 2. Leave on ice for 30 minutes 3. Add PBS and centrifuge 4. Resuspend pellet in 100 µl FITC conjugated goat anti-mouse in detergent buffer with added 4 % dried non-fat milk. 5. Leave on ice for 30 minutes 6. Add PBS and centrifuge 7. Add 700 µl PBS containing Hoechst 33258, PI and RNaseA.	1. Resuspend pellet in 100 µl detergent buffer with added 4 % dried non-fat milk 2. Leave on ice for 30 minutes 3. Add PBS and centrifuge 4. Resuspend pellet in 100 µl detergent buffer with added 4 % dried non-fat milk 5. Leave on ice for 30 minutes 6. Add PBS and centrifuge 7. Add 700 µl PBS containing Hoechst 33258, PI and RNaseA.

APPENDIX 12

Protocol for running and analyzing cell samples with the LSR II

1. The lasers and detectors used for each fluorochrome are shown in appendix 13. Chose these parameters in the experiment setup.
2. Set the threshold at 5.000 for the FSC parameter
3. Set the voltages for the detectors measuring (PE and) FITC to 425.
4. If compensation is needed, calibrating beads are run and the compensation is calculated.
5. Draw a dot plot showing FSC versus SSC. Manipulate the voltages so that the entire cell population is included in the analysis.
6. Draw a dot plot showing area versus width of the Hoechst 33258 signal. Set a gate to discriminate the wanted cell population of singlets from the doublets (A).
7. Draw (a) DNA histogram(s) showing the number of singlet cells versus detected signal from Hoechst 33258 (and PI). Manipulate the voltage(s) until the peak representing G1 cells is localized at channel number 50. Gate for separating the phases G1, S and G2-M (B).
8. For LFM fixed cells: draw a dot plot showing the signal from Hoechst 33258 versus that from PI. Separate the G2 cells from M phase cells (C).
9. For methanol fixed cells: draw a dot plot showing the signal from PE versus that from Hoechst 33258. Separate G2 cells from M phase cells (D).
10. Draw histograms showing the FITC signal (CKS2 protein content) for each phase separately (E). Gate at the peaks for eliminating unwanted contributions.
11. Draw the final hierarchy (F). Use the FITC-A Median numbers for the gated peaks as the measured value for CKS2 protein content in further processing of the data.

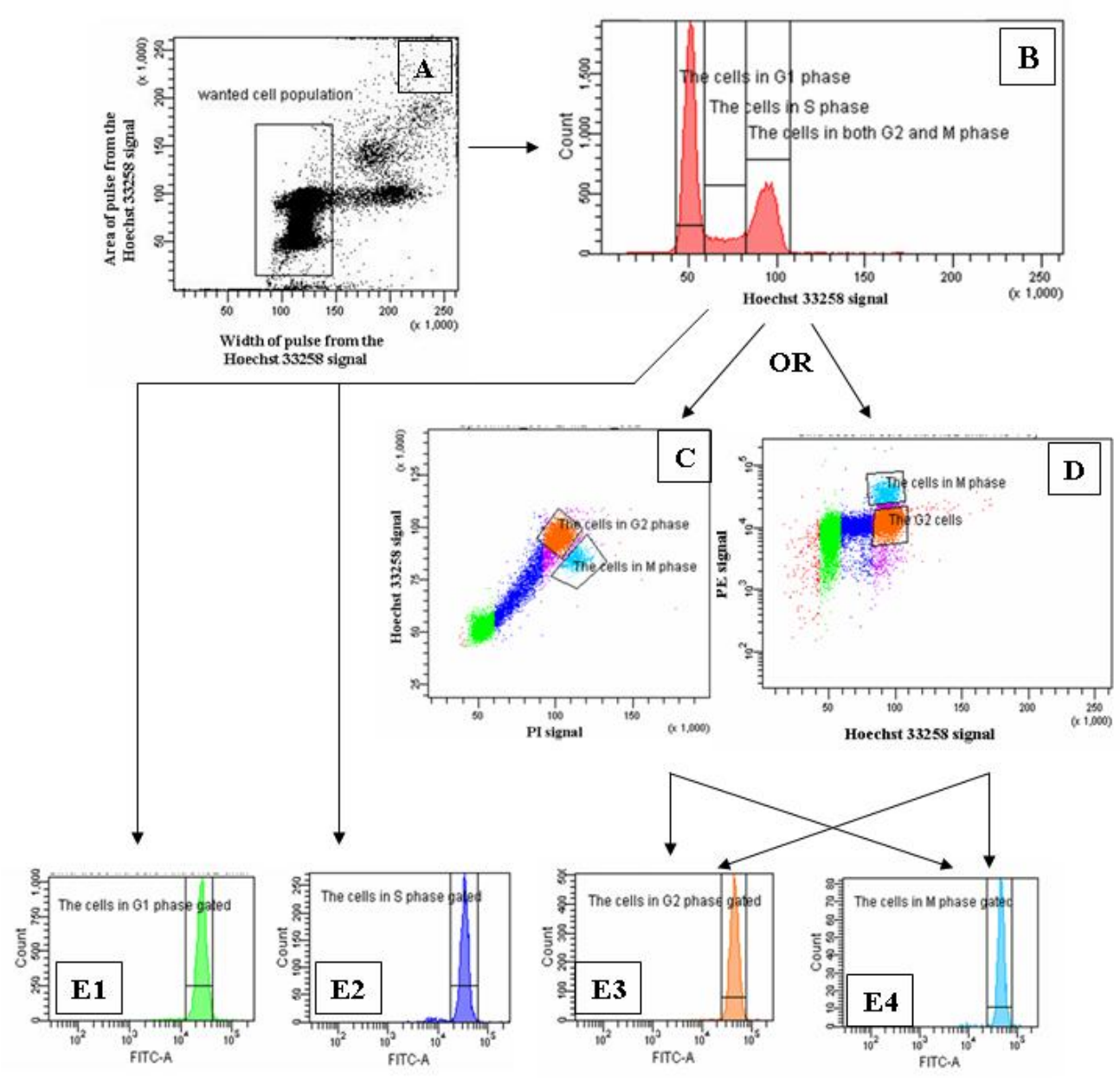

F

Experiment Name:
Specimen Name:
Tube Name:
Record Date:
$OP:
GUID:

Population	#Events	%Parent	FITC-A Median
All Events	30,000	####	31,844
wanted cell population	26,360	87.9	30,515
The cells in G1 phase	14,619	55.5	25,760
The cells in G1 phase gated	14,255	97.5	25,786
The cells in S phase	3,110	11.8	33,738
The cells in S phase gated	2,967	95.4	33,974
The cells in both G2 and M phase	8,248	31.3	44,950
The cells in M phase	831	10.1	47,694
The cells in M phase gated	819	98.6	47,770
The cells in G2 phase	6,455	78.3	44,845
The cells in G2 phase gated	6,407	99.3	44,887

APPENDIX 13

The combinations of fluorochromes, lasers, filters and detectors used for my work

Fluorochrome/ cell quality measured	Cellular component represented by the detected fluorescence	Absorption maximum (nm)	Emission maximum (nm)	Numbers collected from	Laser used	Detector used	Dichroic filters associated with the detector
FSC					Blue (Coherent Sapphire™), 488 nm	Photodiode	
SSC					Blue (Coherent Sapphire™), 488 nm	PMT E in the octagon	BP 488/10
Hoechst * 33258 in H_2O	DNA	345	455	Invitrogen	Ultraviolet 325 nm	PMT B in the trigon	BP 450/50
fluorescein isothiocyanate (FITC)	Cks2 protein	494	519	BD Bioscience	Blue (Coherent Sapphire™), 488 nm	PMT D in the octagon	BP 530/30 LP 505
Phycoerythrin (PE)	cells in M phase	546	578	BD Bioscience	Blue (Coherent Sapphire™), 488 nm	PMT C in the octagon	BP 585/42 LP 550
Propidium Iodide (PI)**	DNA	535	617	Invitrogen	Blue (Coherent Sapphire™), 488 nm	PMT B in the octagon	BP 670/14 LP 635

* The Hoechst fluorochrome binds to DNA in the minor groove with preference for AT rich regions.

** The PI fluorochrome inserts itself between bases with little or no sequence preference with the stoichiometry of one dye pre 4-5 base pairs of DNA. Since PI does not discriminate on sequence or base pairs, it will also bind to RNA. RNaseA must therefore be added. The filters associated with the detector for recording the PI signal block the wavelength where PI has maximum emission. Since PI emits light in a broad range of wavelengths (figure 5 in text), a strong signal will be detected even it the maximum is missed. Therefore this has no practical relevance.

APPENDIX 14

Reagents used in the experiments

Name	Company	Concentration
Dulbecco's Modified Eagles Medium	Sigma	
Dulbecco's PBS without Ca & Mg	PAA	1x
Trypsin-EDTA	Gibco/Invitrogen	1x
Penicillin/Streptomycin	PAA	100x
L-glutamin	PAA	100x
Foetal Bovine Serum	Gibco/Invitrogen	
Polyclonal Goat Anti-Mouse Immunoglobulins/ FITC Goat F(ab')2	DakoCytomation	1 g/l
Polyclonal Rabbit Anti-Mouse Immunoglobulins/FITC Rabbit F(ab)'2	DakoCytomation	0.97 g/l
Goat F(ab')2 Anti-Rabbit IgG (H+L)	Caltag/Invitrogen	0.1 mg/0.5 ml
Methanol	Rathburn	100 %
Formaldehyde Solution	J.T. Baker	37 %
Anti-phospho-Histone H3 (Ser10), Mitosis Marker (rabbit polyclonal IgG)	Upstate	1 µg/µl
Mouse anti-CKS2	Zymed/Invitrogen	0,5 mg/ml
Hoechst 33258	Calbiochem/Merck Biosciences	-
PI	Calbiochem/Merck Biosciences	-
RNaseA	Amersham Biosciences	10 mg/ml